

## **PROJECT ADMINISTRATION**

**R. B. Neal**

In this chapter the organizational structure of SLAC as it evolved during the 4-year design and construction program is discussed. This is followed by an account of the scheduling techniques used by SLAC and by ABA. Finally, fiscal and manpower experiences are recounted.

### **4-1 Organization**

The functional relationships among SLAC, Stanford University, the U.S. Atomic Energy Commission, and the various advisory and coordinating committees were discussed in Section 1-4. It is the purpose of this section to describe the internal organization and functioning of SLAC in somewhat more detail.

The chief executive officer for SLAC is the project director, who reports administratively to the president of Stanford University. The director is assisted in his duties by the deputy director and by a small planning and coordinating staff. In case of prolonged absence of the director, his duties are assumed by the deputy director.

Throughout its existence, SLAC has consisted of four major divisions: the Research Division, the Technical Division, the Business Services Division, and the Administrative Services Division. While these divisions have been continuously in effect, their internal structures have gradually evolved to meet the changing needs of the project as its orientation has turned successively from conceptual design and development to engineering, to procurement and fabrication, to installation and checkout, to operation for accelerator testing and shakedown, and finally to operation for physics research.

Continuity of group effort has been a basic project policy. In general, the same people were involved in all phases of work associated with a given

component or system from early design to final installation, checkout, and test. This same policy has continued into the operating period so that many staff members have had an unbroken association with a particular component or system through the entire span of its conceptual and physical existence. One of the merits of this policy is its salutary effect on quality at each step through the program. This results from the continuing awareness of each staff member that tomorrow he will be required to face the consequences of today's decisions and actions. Another worthwhile result of this policy has been the breadth of experience which staff members have gained during exposure to the various phases in the evolution of a component or system. From another point of view, it can be stated with some conviction that the continuity policy being discussed influenced the project in its choice of staff. Each new member was chosen not just for his ability to design, or fabricate, or install, but to do all of these things and later play a creative and productive role during the operating phase of the laboratory.

In addition to promoting a high degree of efficiency and responsibility as discussed above, this general expectancy of personnel continuity has been an important factor in the maintenance of personnel morale during the 5 years SLAC has been in existence.

The organization of the project as it existed in January 1962 (3 months after Congressional authorization) is shown in Fig. 4-1 with the number of personnel in each group indicated in its box. The total staff at that time numbered 200, classified as shown in Table 4-1. The "professional" category

Figure 4-1 Project organization as of January 1962.

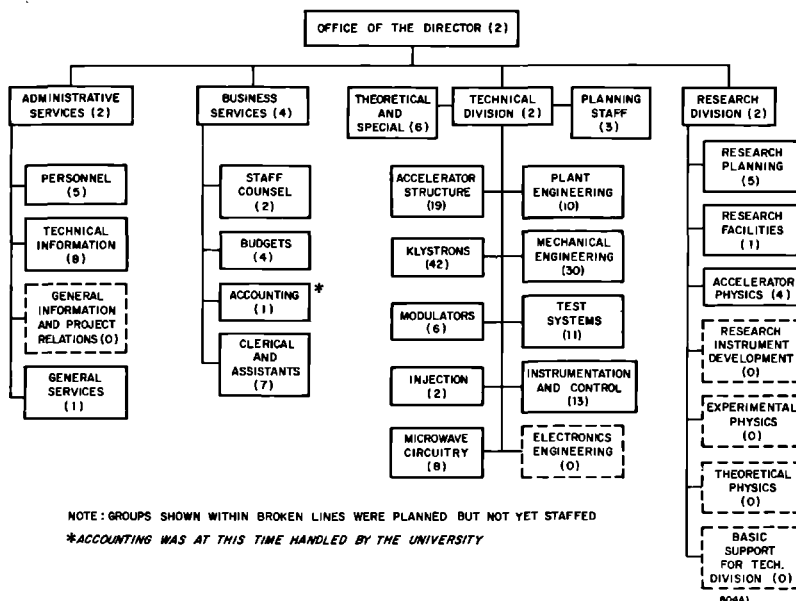


**Table 4-1 Classification of SLAC staff (January 1962)**

<i>Division</i>	<i>Professionals</i>	<i>Technicians</i>	<i>Draftsmen</i>	<i>Clerical</i>	<i>Total</i>
Director's Office	1	—	—	1	2
Research	11	—	—	1	12
Technical	60	66	16	10	152
Business Services	6	—	—	12	18
Administrative Services	7	—	—	9	16
	85	66	16	33	200

included all people with college degrees. By that date, the Technical Division had already undergone a rapid expansion and, as indicated in Fig. 4-1, the organization of this division had a strong orientation toward component and systems development. The Klystron Group was the largest group at that time, reflecting the fact that the project had put strong emphasis on klystron development during the preauthorization period. The Microwave Circuitry Group had the responsibility for development of the basic parameters of the accelerator structure and for the design of the RF drive and phasing systems. The Accelerator Structures Group was responsible for the design and fabrication of the disk-loaded accelerator tube and the rectangular waveguide system. The Plant Engineering Group was responsible for technical liaison between SLAC and Aetron-Blume-Atkinson, the architect-engineering-management organization under contract to SLAC for the design of the conventional buildings and facilities (including the accelerator housing and the klystron gallery, the beam switchyard, and the research area buildings). The Mechanical Engineering Group was responsible for layout of the various accelerator systems in the accelerator housing and klystron gallery and for engineering of the cooling water, electrical, and support systems within these structures. All project drafting was centered in this group, but provisions were made for assignment of draftsmen to other groups as required. The Test Systems Group included personnel associated with the 75-MeV Mark IV accelerator which was used as a vehicle for testing prototype components of the two-mile accelerator. In January 1962, planning of the beam switchyard and the research area had barely started. Some preliminary thinking concerning these areas had begun in the Research Planning Group within the Research Division.

Two years later, in March 1964, the SLAC organization was as shown in Fig. 4-2. By this time the project was roughly halfway through the construction period and the total SLAC staff had reached the level of 731, as shown in Table 4-2. A number of organizational changes had taken place since January 1962 (Fig. 4-1) and are shown in Fig. 4-2. The title of the Accelerator Structures Group had been changed to the Mechanical Design and Fabrication Department. This department was responsible for all project machine shops

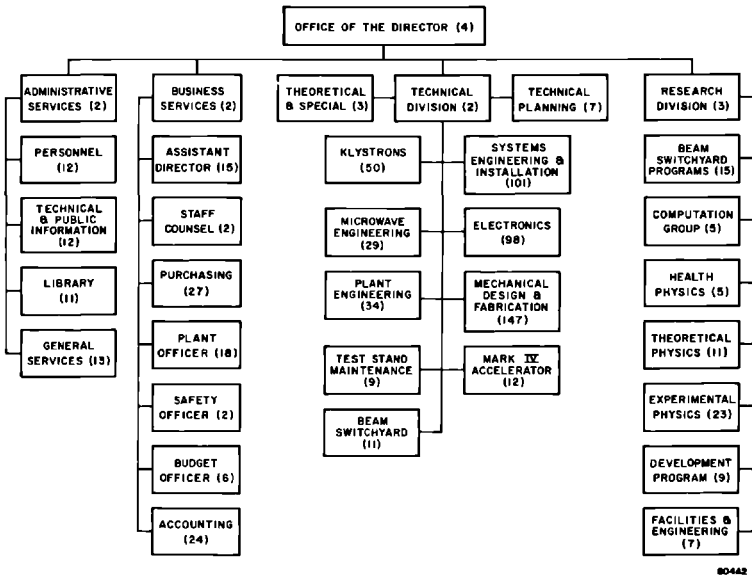


Figure 4-2 Project organization as of March 1964.

as well as for fabrication of the disk-loaded accelerator and the rectangular waveguide system. Mechanical engineering was also centralized in this department although a number of mechanical engineers were on assignment to other Technical Division groups and to the Research Division. The title of the former Mechanical Engineering Group shown in Fig. 4-1 was changed to the Systems Engineering and Installation Department. The responsibilities of the Microwave Engineering Group now included the injector system. A new *ad hoc* group responsible for the beam switchyard was now in existence. An Electronics Department consisting of Heavy Electronics, Light Electronics, and Instrumentation and Control Groups had been formed.

This is perhaps a good time to discuss another policy which has been in effect, with a few exceptions, since the project was initiated. The Technical Division has been responsible not only for the design and construction of the

Table 4-2 Classification of SLAC staff (March 1964)

<i>Division</i>	<i>Professionals</i>	<i>Technicians</i>	<i>Draftsmen</i>	<i>Clerical</i>	<i>Total</i>
Director's Office	2	—	—	2	4
Research	43	26	—	9	78
Technical	149	268	55	31	503
Business Services	13	16	—	67	96
Administrative Services	6	—	—	44	50
	213	310	55	153	731

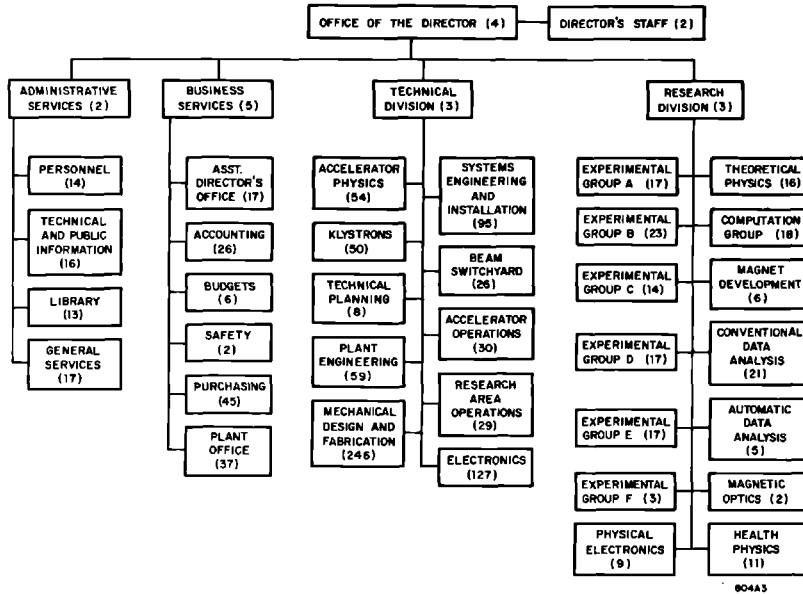


Figure 4-3 Project organization as of January 1966.

accelerator (and more recently for the operation of the accelerator and the research area facilities) but also for the technical support of the Research Division. This support has consisted of supplying machine shop and electronics shop services, and mechanical and electronics engineering and technician assistance. At the option of the customer group, the engineering and technician assistance can be given on a short-term or long-term personnel loan basis or by undertaking the job assignment within the support group itself. Both methods have been found to be effective.

The project organization in January 1966 is shown in Fig. 4-3. The total head count at that time was 1115 which was not far below the peak number reached during the construction period. The staff was divided as shown in Table 4-3.

Table 4-3 Classification of SLAC staff (January 1966)

<i>Division</i>	<i>Professionals</i>	<i>Technicians</i>	<i>Draftsmen</i>	<i>Clerical</i>	<i>Total</i>
Director's Office	4	—	—	2	6
Research	85	81	—	16	182
Technical	190	433	71	33	727
Business Services	27	59	—	52	138
Administrative Services	17	—	—	45	62
	323	573	71	148	1115

Six experimental groups had been activated in the Research Division. In the Technical Division, two operations groups, Accelerator Operations and Research Area Operations, had been formed and were vigorously preparing for beam turnon, scheduled to occur a few months later. A new department, Accelerator Physics, comprising the former Microwave Engineering Group, the Instrumentation and Control Group (previously in the Electronics Department), and the Theoretical and Special Group, was in effect. Other responsibilities then belonging to Accelerator Physics were magnetic measurements and the laser alignment system.

The final chart, Fig. 4-4, represents SLAC as it existed in July 1967. By this time, the machine had been operational about 14 months and the physics research program had been underway about 8 months. The number of separate organizational entities in the Technical Division had been reduced to eight. The completion of the activities of ABA and the completion of accelerator and beam switchyard installation and checkout resulted in a reduction in the scope of work for both the Plant Engineering and the Systems Engineering and Installation Departments. Therefore, it was possible to combine both of these into one department which was called Plant Engineering. Because the activities of the *ad hoc* Beam Switchyard Group were completed, this group was disbanded and its members were returned to their home groups or were reassigned to other work. Some of the key people from this group were combined with the Research Area Operations Group into a new department called the Research Area Department. The responsibilities of this department

Figure 4-4 Project organization as of July 1967.

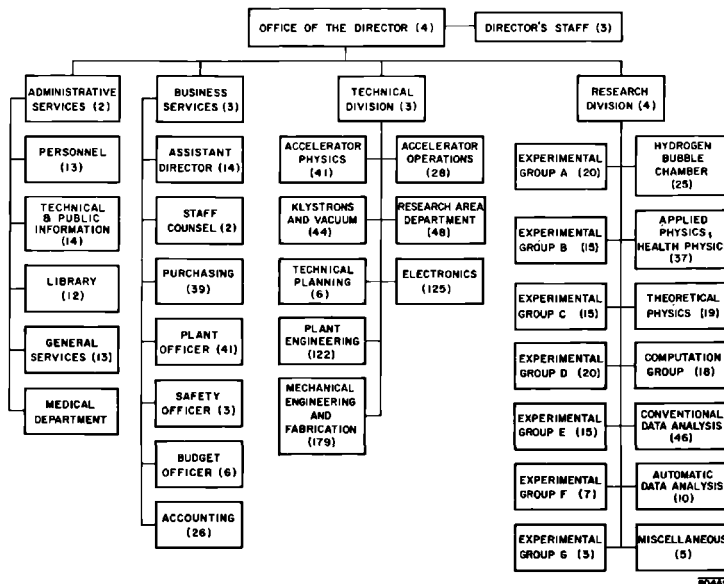


**Table 4-4 Classification of SLAC staff (July 1967)**

<i>Division</i>	<i>Professionals</i>	<i>Technicians</i>	<i>Draftsmen</i>	<i>Clerical</i>	<i>Total</i>
Director's Office	5	—	—	2	7
Research	110	86	—	63	259
Technical	165	350	54	26	595
Business Services	18	74	—	42	134
Administrative Services	12	16	—	26	54
	310	526	54	159	1049

include operation and maintenance of the beam switchyard, experimental beam planning, and construction and logistics in the research area. The responsibility for the accelerator vacuum system was transferred from the Systems Engineering and Installation Department to the Klystron Group. The name of this department then became the Klystron and Vacuum Department.

By July 1967, the project staff had decreased from the peak level of about 1200 in fiscal year (FY) 1966 to a total of 1049. It was expected that the staff would remain approximately at this level for the next year. The staff was divided as shown in Table 4-4.

## 4-2 Scheduling

When the SLAC project was initiated, it was recognized that the timely completion of the entire program of design and construction required the successful coordination of contributions from many individuals and organizations representing a broad spectrum of trades and disciplines. Moreover, it was clear that meeting the project's overall schedule required that much of the work proceed in a concurrent manner, e.g., the design and construction of the facilities had to be carried out in parallel with the development of criteria for the accelerator and research equipment. The mutual interaction of these key project elements required that a scheduling technique capable of dealing logically and expeditiously with the various interdependent factors and constraints be employed.

After considering several scheduling techniques, the critical path method (CPM) was selected as the most appropriate system. It was used by both SLAC and ABA during the entire design, construction, installation, and checkout phases of the project.

A basic CPM diagram shows the activities of a project arranged in logical sequences. An *activity* is a task or operation which can be clearly defined and for which a single responsibility can be assigned for its execution. Activities are separated by *event nodes* (which are merely numbered circles on the CPM diagram). Arrival at a node signifies completion of the previous activities

leading to the node and readiness to undertake the activities beyond the node. A sequence of activities and nodes from the start to the finish of a project is a *path* through the project. Usually, there are a number of parallel paths each representing a chain of activities associated with the accomplishment of a major phase of the project. Often, it is not feasible to proceed with a particular activity, A, along a certain path until other activities, say, D, F, G, associated with one or more different paths have first been accomplished. In this situation, the undertaking of activity A is said to be *restrained* by activities D, F, G.

The complete CPM logic diagram is first made up without paying attention to the time required for the various activities. After completion of the diagram, the time required for the accomplishment of each activity is then entered on the diagram opposite that activity. The times for each path are then summed up taking into account the various restraints. The path requiring the maximum total time is called the *critical path*. It is clearly the path that defines the time required to complete the entire project. Activities that are not on the critical path can start late and still finish by the time the critical path activities are completed. The amount of extra time available to complete an activity without delaying the overall schedule is called the *float time* for that activity. It is the difference between the time available for an activity and its nominal duration. From this discussion, it is evident that activities on the critical path have zero float times.

Several particular advantages accrue from the use of CPM scheduling (or other similar techniques). The interrelationships of the various activities comprising an entire project are clearly revealed. The critical items which determine the duration of the entire project are identified. Thus, any improvement in schedule requires a reduction in duration of one or more of these critical activities. Actual status of the project can easily be compared with scheduled status at any point in time during the program. The effects on total schedule of changing the logic of the CPM network or changing the durations of some of the activities can be quickly ascertained.

Calculation of the early and late starting times, the early and late finishing times, and the float times for the CPM networks can be accomplished either manually or by machine. With complex networks, the computer offers the advantages of speed, accuracy, and the ability to sort activities, e.g., by responsibility or by starting time.

The completed CPM network is basically a logical plan for accomplishing a given project. It provides indications of the proper priorities to be placed on such matters as the delivery of materials, the allocation of manpower, and the utilization of tools and equipment in order to achieve an overall schedule. By revealing which activities are on the critical path, the CPM indicates where extra manpower, overtime, or expediting should be brought to bear or where an alternative or parallel solution should be sought. It simultaneously reveals the activities with float times where extra efforts will not improve the overall schedule, but where, indeed, some relaxation in efforts may be feasible.



The use of a new scheduling technique in a complex program such as that at SLAC required that large numbers of key individuals associated with SLAC, ABA, and the AEC receive training in these methods. CPM classes were held and information was disseminated to promote a common understanding of the terminology, procedures, and interpretation of this scheduling technique. In many cases, SLAC and ABA personnel also trained members of subcontracting firms in the application of CPM.

The critical path method was utilized throughout the SLAC construction period and proved to be useful for setting up and controlling schedules. CPM continues to be used during the operating period.

During the design, construction, installation, and checkout phases, a status review meeting with one of the Technical Division groups was conducted by the Division Head each morning. The number of groups was such that each group was reviewed once every 2-weeks on a regular basis. At each of these meetings, a detailed independent report of group progress measured against the CPM schedule was presented by a member of the Technical Planning Department. Lagging activities were promptly identified and corrective steps were initiated. In some cases, alternative or "backup" programs were mounted. The status reports not only reviewed the progress of in-house work but also the progress of subcontracted components and materials. Regular visits to the plants of subcontractors were made by members of the responsible technical groups. When potential problems were recognized, the subcontractors were immediately informed of SLAC's concern, and meetings to seek possible solutions were held. If doubts persisted even after these actions were taken, separate parallel subcontractual arrangements were considered and in those cases where the overall program appeared to be threatened, these parallel programs were undertaken.

### 4-3 Fiscal experience

Financial support of SLAC has come principally from three funds administered by the U.S. Atomic Energy Commission: (a) a \$18.1 million preconstruction research and development (R and D) fund; (b) a \$114 million design and construction fund authorized by Congress in September 1961; and (c) a preoperation R and D fund totaling \$26.7 million through FY 1966. The latter fund changed character from "preoperations" to "operations" starting in FY 1967. Expenditure rates for each of these funds are shown in Fig. 4-5.

Expenditures under the preconstruction R and D fund started in January 1961, about 9 months in advance of construction authorization. This work was initially a continuation of earlier R and D activities on accelerator structures and associated components already being supported by the AEC at the Hansen Laboratories. The expenditure of preconstruction R and D funds continued over a 5½ year period, reflecting the fact that the development activities associated with some of the components for the accelerator

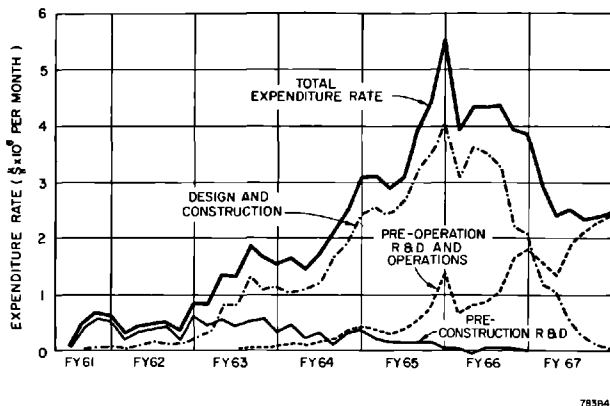


**Figure 4-5 Expenditure rates for preconstruction research and development, design and construction, and preoperation research and development funds.**

were completed and the designs frozen early while the development of other components and systems, particularly those utilized in the beam switchyard and research area, could not start until the programs and conceptual designs of these areas were formulated. Such considerations, stemming from the diversified nature of the accelerator and its associated research facilities, explain why the preconstruction R and D program extended through almost the whole of the construction period, although its scope was considerably diminished during the 2 final years.

Expenditure of construction funds began in March 1961, about 7 months in advance of construction authorization. The early expenditures consisted principally of money advanced by the AEC to support master planning of the accelerator site, buildings, and utilities.

This preliminary planning was very important in enabling the project to get off to a fast start after the contractual agreement between Stanford and the AEC for construction of the two-mile accelerator was reached in April 1962. For example, initial ground breaking at the accelerator site took place on July 9, 1962, and actual construction of the first two buildings, the Test Laboratory and the Administration-Engineering Building, commenced on August 2, 1962, and September 25, 1962, respectively.

In FY 1963, the construction costing rate began to increase rapidly. It continued to climb during FY 1964 and 1965, reaching a peak rate of approximately \$4 million/month early in FY 1966. The rate declined rapidly after that but remained finite for some time because of modifications and extensions of facilities and settlement of contractor claims.

The number of procurement actions, i.e., subcontracts, purchase orders, and change orders per 6-month period is plotted in Fig. 4-6. These actions reached a maximum rate of approximately 2000 per month in late FY 1966. The corresponding costs incurred during each 6-month period are also shown in Fig. 4-6 for SLAC only and for SLAC plus ABA. Note that the SLAC cost

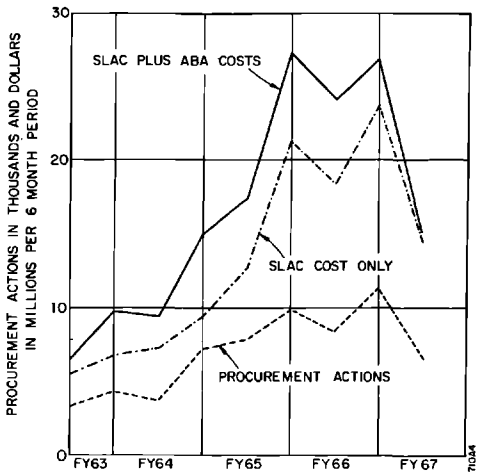


Figure 4-6 Number of procurement actions and associated costs.

rate reached a peak about 1 year after the peak of ABA's cost rate.

The integrated overall project construction costs and costs plus commitments versus time are shown in Fig. 4-7. These are in the form of classical "lazy S" curves applicable to most construction projects. These curves represent the sum of SLAC and ABA costing experiences.

The breakdown of the \$114 million construction budget into the principal categories of engineering, design, inspection, and management (EDI and M), direct construction, indirect costs, and escalation and contingency is shown in Table 4-5. For comparison, these costs are given for two points in time: November 1962, shortly after the systems criteria were established and preliminary designs completed; and July 1967, when construction was substantially completed. At the earlier date, the escalation and contingency

Figure 4-7 Integrated total costs and commitments for overall SLAC construction project.

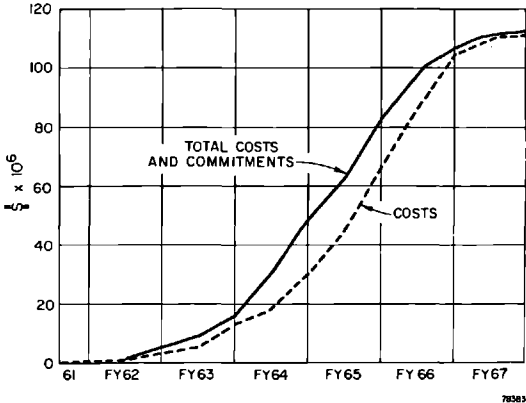


**Table 4-5 Accelerator construction costs**

<i>Construction categories</i>	<i>11/1962</i>	<i>7/1967</i>
EDI & M	\$ 7,907,800	\$ 13,804,835
Direct construction :		
Improvements to land	1,476,000	2,296,388
Buildings	18,778,900	24,850,066
Utilities	7,575,400	8,099,034
Equipment	6,121,200	5,759,781
Modulators	8,332,500	4,645,641
RF Systems (phase/drive)	2,197,200	2,026,807
Accelerator structures	6,326,000	6,945,585
Electrical system	1,117,400	1,605,565
Mechanical systems	5,619,500	5,965,380
Injection system	357,500	599,498
Instrumentation and control	4,295,800	4,821,827
Klystrons	2,496,000	3,392,785
Test stands (constr. and operation)	2,126,700	1,992,467
Beam switchyard equipment	2,624,500	8,538,593
End station equipment	2,436,000	2,880,463
1-meter Hydrogen bubble chamber		19,345
Total direct construction	\$ 71,880,600	\$ 84,539,225
Indirect Costs	11,392,300	15,404,003
Subtotal	\$ 91,180,700	\$113,748,063
Reserve for Escalation & Contingency	22,819,300	251,937
Total	\$114,000,000	\$114,000,000

reserve was kept intact and was not apportioned to the systems and components budgets in advance of proven needs for these funds. In fact, this policy was followed throughout the construction program. As can be seen in Table 4-5, the cost of EDI and M, the cost of twelve of the direct construction items, and indirect costs increased during this period. On the other hand, the cost of four of the direct construction items decreased. The reasons for these changes upward and downward include poor initial estimating, changes in scope, and changes in local or national labor or materials costs. The relative weight of these factors varied from system to system and will not be given here. From the subtotal, it may be noted that the total project estimated cost increased about 25% during the 4-year construction period. Fortunately, it was possible for this increase to be completely absorbed by the escalation and contingency reserve. The major cost increases occurred in the cases of those items (a) on which little previous experience was available and (b) for which design of prototypes was not feasible (e.g., large-one or few-of-a-kind devices such as those located in the beam switchyard) or not possible because of time limitations. Where these factors were not present, the early cost

estimates proved to be remarkably good and the increases which occurred could largely be attributed to escalation. Thus the cost of conventional construction and of the accelerator proper was kept very close to original estimates. The factors enumerated above as causes of cost increases apply principally to the beam switchyard and the target areas. Evolution of new knowledge in the areas of physics on which the accelerator was to have its maximum impact, has changed concepts of the beam switchyard and the target areas considerably from those envisaged in the original proposal, and the talent necessary to inject this new information into design concepts was not available in the earliest phases of the project. As a result it can be stated that almost the entire contingency allocated to the project has been used in those areas directly associated with the specific physical research program envisaged for the accelerator.

Schedule and cost information for the principal SLAC buildings and structures is shown in Table 4-6. This table gives the starting and completion

**Table 4-6 Principal SLAC buildings and structures**

<i>Name</i>	<i>Date construction started</i>	<i>Date of completion</i>	<i>Construction cost (dollars)</i>	<i>Gross area (sq. ft)</i>	<i>Cost (dollars/sq. ft)</i>
Test Laboratory	8/62	6/63	910,831	41,500	22
Administration- Engineering Bldg.	9/62	9/63	787,740	44,023	18
Construction Office Bldg.	12/62	6/63	188,305	15,000	13
Electronics Bldg.	2/63	11/63	341,238	26,500	13
Fabrication Bldg.	2/63	12/63	778,452	32,250	24
Accelerator Housing	6/63	10/64	4,727,632	154,355	31
Klystron Gallery	10/63	6/65	3,630,167	361,483	10
Central Laboratory	12/63	4/65	1,582,345	60,275	26
Heavy Assembly Bldg.	12/63	10/64	764,469	34,850	22
Control Bldg.	6/64	3/65	288,332	13,842	21
Beam Switchyard and D.A.B.	9/64	3/66	4,394,792	58,256	75
Cafeteria and Shop Dining Room	1/65	8/65	129,844	4,875	27
Auditorium	1/65	8/65	186,620	7,550	25
End Station A and Beam Dump East	3/65	7/66	2,623,107	32,388	81
End Station B	3/65	7/66	987,978	17,000	58
Cryogenics Bldg.	9/65	5/66	295,749	8,000	37
Fire Station	5/67	1/68	95,880	2,590	37
General Services Bldg.	12/67	8/68	543,200	30,419	18
Central Laboratory Addition	12/67	11/68	822,000	30,900	27

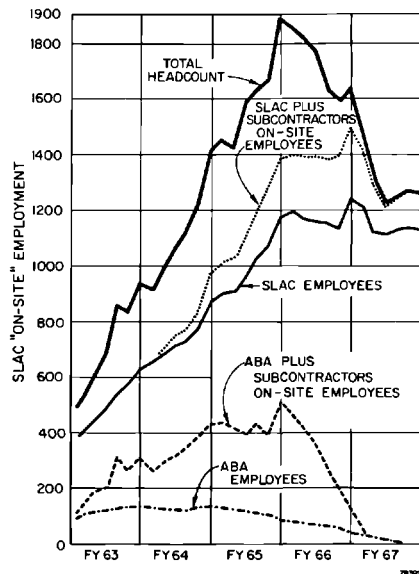
dates of each facility, the total construction cost, the gross area, and the cost per square foot. Engineering, design, inspection, and management costs are not included in this table. It may be noted that the cost per square foot ranged between \$10 and \$85 for the various structures. Altogether, the total gross area listed in the table is 976,056 sq ft at an average cost of \$24.67/sq ft.

#### 4-4 Manpower

The total manpower involved in the design, construction, and operation of SLAC, including the accelerator, buildings, and facilities, is shown in Fig. 4-8. The lower curve shows the manpower associated with ABA. The second curve from the bottom gives the total of ABA employment plus their subcontractors' on-site personnel. ABA reached a manpower peak of about 140 at the end of FY 1963 and then began a gradual phaseout over a 3½ year period. On the other hand, the manpower of ABA's subcontractors did not reach a peak until early in FY 1966 and then declined rather rapidly over a 1-year period.

Direct SLAC employment and the total of SLAC plus its subcontractors' onsite employees are shown, respectively, in the third and fourth curves from the bottom of Fig. 4-8. The bumps on the SLAC curve at the beginning of FY 1965, 1966, and 1967 represent student summer employment (typically about 60 to 75). The upper curve in Fig. 4-8 represents the total employment at the SLAC site. It reached a peak of about 1900 in July 1965. Direct SLAC employment in terms of man-months of effort is shown in the upper curve of Fig. 4-9. This plot is similar to the center curve of Fig. 4-8 but reflects the effects of vacations, overtime, and the exclusion of summer employment.

**Figure 4-8 SLAC "on-site" employment.**



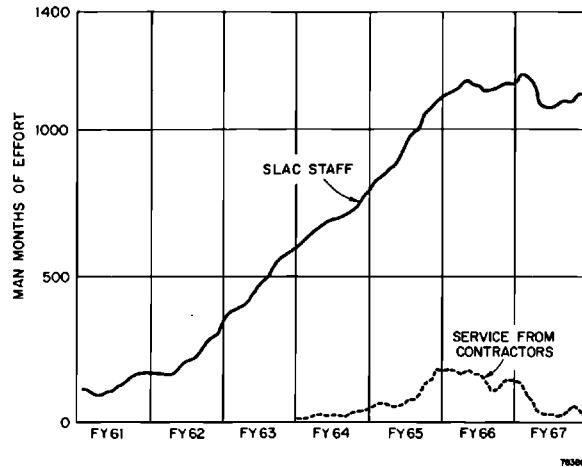


**Figure 4-9 SLAC staff effort and services from contractors.**

The direct SLAC effort started with a nucleus of about 30 people of all classes from the W. W. Hansen Laboratories at Stanford University. A serious effort was made to avoid excessive buildup of the long-term SLAC staff during the periods of peak manpower demand. In general, it was the intent to acquire staff members who would participate not only in the design and construction phases of the project but who would also remain as effective, continuing staff during the operating and research phases. While complete success in carrying out this objective was not achieved, the upper curve of Fig. 4-9 shows a reasonable approach to this goal. Methods used to control direct SLAC staff buildup included: (a) the hiring of approximately 140 people with appointments terminating at the end of construction (up to 6 weeks' termination pay was stipulated in the offer of employment provided the worker remained until his employment was terminated by SLAC), (b) the use of engineering services from outside engineering firms, contract draftsmen and designers, and several outside "captive" machine shops. These contract services, which reached a peak level of approximately 180 people, extended over the period from FY 1964 through 1967 as shown in the lower curve of Fig. 4-9.

The SLAC man-month effort reached a peak of 1170 in October 1965, and remained approximately constant at this level until August 1966, when it began to decline slowly. A drop to 1049 by July 1967 resulted. During FY 1965 and 1966 the project monthly turnover rate averaged about 2%. The rate was lower than this figure prior to FY 1965 and higher (up to 4% per month) during the first half of FY 1967 as the end of the construction phase approached. During the latter period, the high turnover resulted in part from the dismissal of a substantial portion of the employees with temporary appointments. A few of the latter class of workers proved to be so effective that they were offered permanent positions.





## **GENERAL DESCRIPTION OF SLAC AND TWO-MILE ACCELERATOR**

**R. B. Neal**

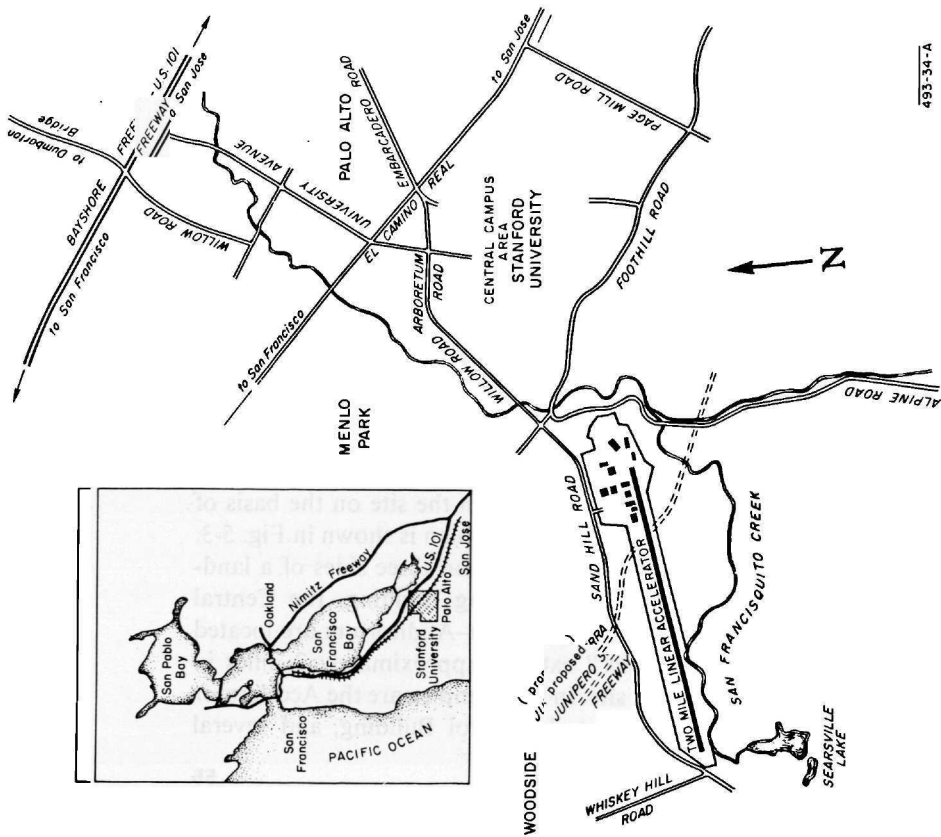
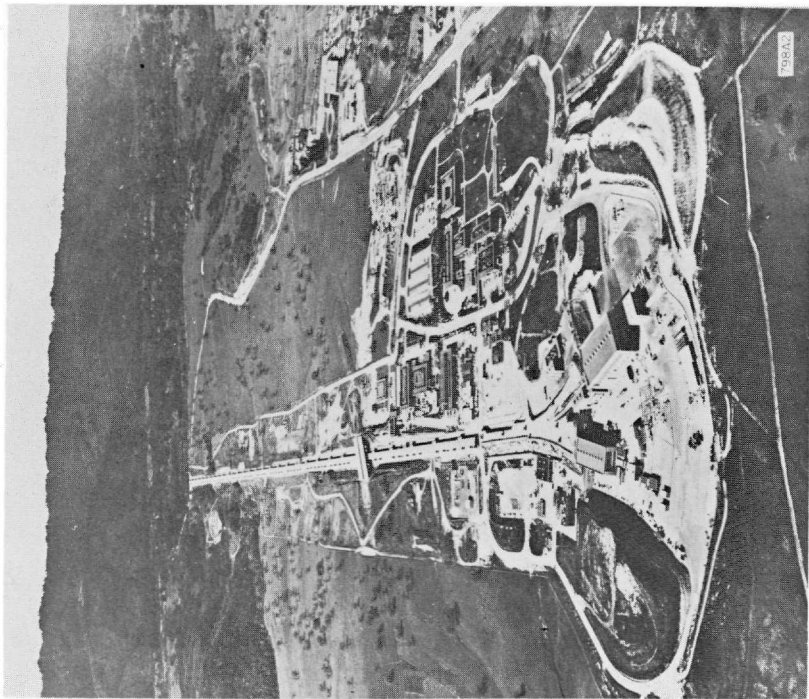
This chapter presents an overall preliminary description of the accelerator site and the principal systems and components of the two-mile accelerator. More complete accounts of these systems and components are given in later chapters. In addition, accelerator performance and operating statistics obtained during the first year of operation are presented.

### **5-1 Description of site, principal buildings, and laboratories**

The Stanford Linear Accelerator Center is located on 480 acres of land about 2 miles west of the main Stanford campus. The location of the site relative to the University and the surrounding communities is shown in Fig. 5-1. In Fig. 5-2, an air view of the site shows the research area in the foreground, the principal laboratories, offices, and shops in the center, and the accelerator and klystron gallery running west to east (top to bottom in the photograph). The injector is located at the west end of the accelerator (top of the photograph). The site is 1000 ft wide along most of the accelerator length. It increases to about 3000 ft at the target end to allow space for buildings and experimental facilities.

In the general plan for SLAC, the buildings are arranged into four major divisions. The facilities and structures are located on the site on the basis of their specific functions and interrelationships. A site plan is shown in Fig. 5-3. The "campus area" consists of buildings arranged on three sides of a landscaped open mall. The Administration-Engineering Building, the Central Laboratory, the Test Laboratory, and the Cafeteria-Auditorium are located in this area. The "accelerator complex" extends approximately 2 miles in length and traverses most of the SLAC site. In this complex are the Accelerator Housing, the Klystron Gallery, the Central Control Building, and several

Figure 5-2 Air view of SLAC site showing the two-mile accelerator, the research facilities, and the principal laboratories and shops.



493-34-A

Figure 5-1 Site location relative to Stanford University and surrounding communities.

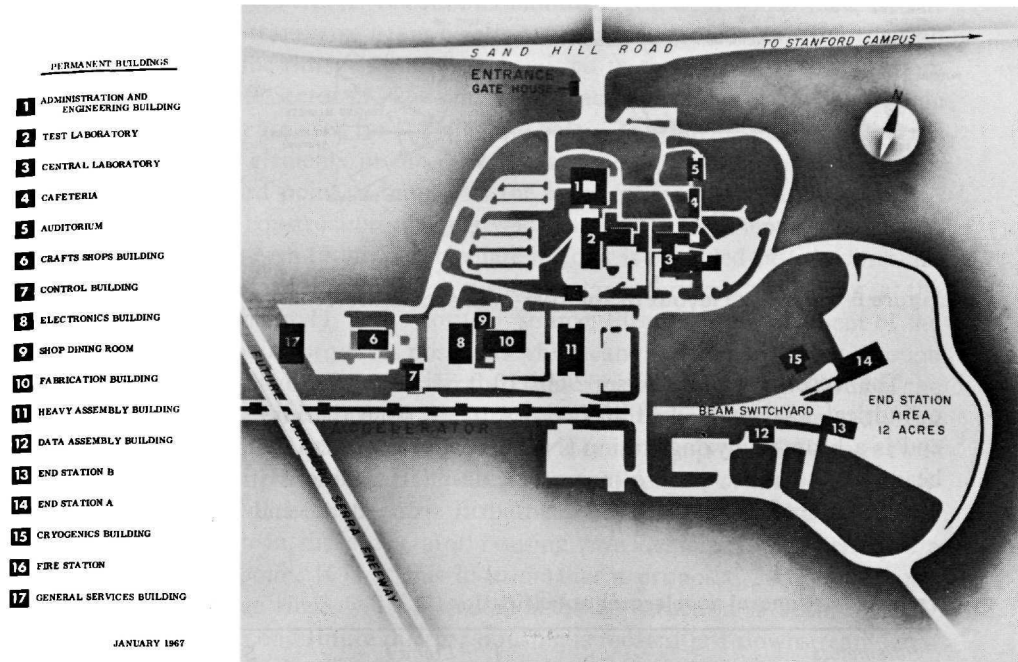


Figure 5-3 Site plan.

related electrical power, cooling water, instrumentation, and utility structures. The "support complex" is situated between the campus area and the accelerator. It includes the Fabrication Building, Heavy Assembly Building, Electronics Building, General Services Building, Fire Station, storage yards, and general service structures and facilities. These structures are located so as to be easily accessible from other areas of the project requiring their services. The "research area" occupies the eastern end of the site. Included in this area are the Beam Switchyard, End Stations A and B, "Counting House," Data Assembly Building, Cryogenic Building, and several related electrical power and utility structures.

## 5-2 General plan of accelerator

A diagram illustrating the entire two-mile accelerator is shown in Fig. 5.4. The overall specifications of the accelerator are given in Table 5-1. The accelerator has been authorized and built in accordance with the Stage I (20-GeV) specifications. Provisions have been made in the design to permit later expansion to Stage II (40 GeV) by connecting additional RF sources along its length. If desirable, the energy increase can be accomplished in an incremental manner.

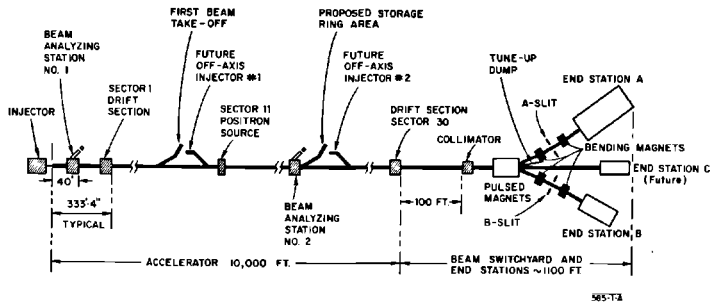


Figure 5-4 Overall layout of the two-mile accelerator.

The accelerator comprises 960, 10-ft sections of 10.5-cm disk-loaded cylindrical waveguide. Just 40 ft downstream from the injector at the west end is a beam-analyzing station (No. 1) which is used to set up the injected beam and to make precise measurements of its characteristics. An instrumentation section is located in a 9-ft drift space at the end of each 333-ft

Table 5-1 General accelerator specifications

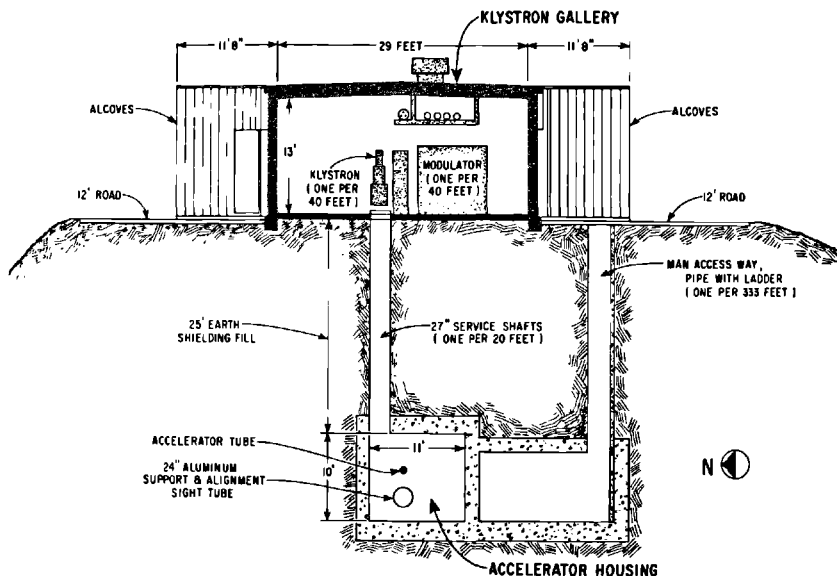
Parameters	Stage I	Stage II
Accelerator length	10,000 ft	10,000 ft
Length between feeds	10 ft	10 ft
Number of accelerator sections	960	960
Number of klystrons	245	960
Peak power per klystron	6–24 MW	6–24 MW
Beam pulse repetition rate	1–360 pulses/sec	1–360 pulses/sec
RF pulse length	2.5 $\mu$ sec	2.5 $\mu$ sec
Filling time	0.83 $\mu$ sec	0.83 $\mu$ sec
Electron energy, unloaded	11.1–22.2 GeV	22.2–44.4 GeV
Electron energy, loaded	10–20 GeV	20–40 GeV
Electron peak beam current	25–50 mA	50–100 mA
Electron average beam current	15–30 $\mu$ A	30–60 $\mu$ A
Electron average beam power	0.15–0.6 MW	0.6–2.4 MW
Electron beam pulse length	0.01–2.1 $\mu$ sec	0.01–2.1 $\mu$ sec
Electron beam energy spread (max)	0.5%	0.5%
Positron energy	7.4–14.8 GeV	14.8–29.6 GeV
Positron average beam current <sup>a</sup>	0.45 $\mu$ A	0.45 $\mu$ A
Multiple beam capability	3 interlaced beams with independently adjustable pulse length and current	
Operating frequency	2856 MHz	2856 MHz

<sup>a</sup> For 100 kW of incident electron beam power at positron source located at one-third point along accelerator length.

sector of the accelerator. It contains monitoring devices which measure the beam current, transverse beam position, and beam profile. This information from each of the thirty sectors is transmitted to the Central Control Room located opposite Sector 27. The same drift space also contains the quadrupole doublets which are used for focusing the beam. These drift space components are important elements in the overall instrumentation and control system. At the one-third point, a branch in the accelerator housing is provided to allow future construction of a reduced-energy experimental facility. A structure to house a future intermediate injector is provided just downstream from the beam takeoff point. Only a short distance farther downstream, at the beginning of Sector 11, is the positron source. Electron bombardment of the target at this point produces positrons which can then be accelerated through the remaining length of the accelerator, thus achieving up to two-thirds of the maximum electron energy. At the two-thirds point is located beam-analyzing station No. 2. This station permits testing a beam of up to 3 GeV over two-thirds of the length of the machine without involvement of the beam switchyard at the end of the accelerator. Just downstream from the analyzing station, another branch in the accelerator housing provides a second intermediate beam takeoff point. It is at this location that a proposed 3-GeV electron-positron storage ring<sup>1</sup> will be located if its construction is authorized by Congress. A second future injector housing is located just downstream from the storage ring takeoff.

A view of the cross section of the accelerator housing and the klystron gallery is shown in Fig. 5-5. These structures are separated by 25 ft of earth

Figure 5-5 Cross section of accelerator housing and klystron gallery.



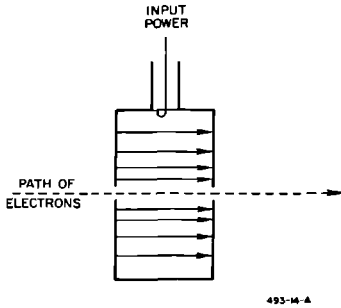


**Figure 5-6**  
Single cavity accelerator.

for radiation shielding. Service shafts, 27 in. in diameter and spaced 20 ft apart, allow passage of waveguides, vacuum manifolds, cooling water piping, and instrumentation cables between the two housings. Man accessways are provided between the two levels at 333-ft intervals along the machine.

### 5-3 Elementary principles of operation

Before describing the two-mile accelerator in more detail, it may be beneficial to give a brief and rather elementary review of the operating principles of linear accelerators.

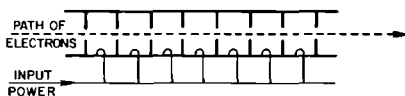
Consider a single cylindrical cavity oscillating in the  $TM_{010}$  mode at a very high (microwave) frequency, as shown in Fig. 5-6. Assume that small holes are made in the centers of the end plates and that a beam of low-energy electrons is shot in through one hole and out the other. Those electrons that pass through the cavity during accelerating phases will gain in energy by the line integral of the electric field along their path. Neglecting transit time considerations, the maximum energy gained will be

$$V = \sqrt{PR}$$

where  $P$  is the RF power dissipated in the cavity and  $R$  is the shunt impedance of the cavity which is defined by this relation.

Now suppose that instead of having a single cavity,  $n$  such cavities are placed end-to-end with the small holes aligned as shown in Fig. 5-7, so that

**Figure 5-7**  
Multiple cavity accelerator.



the beam can pass through. Let the cavities be excited from a transmission line which has its phase velocity adjusted so as to equal the velocity of the accelerated electrons. Then, if the available power is the same as before and equal amounts of power are distributed to each of the  $n$  cavities, the total energy gained will be

$$V = n \left( \frac{P}{n} R \right)^{1/2} = (nPR)^{1/2}$$

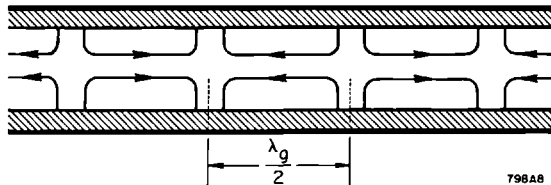
where perfect phasing conditions have been assumed and the transit time effect has again been neglected. This simple example illustrates a basic principle of the linear accelerator: by distributing the available power to  $n$  cavities, the net energy gain has been improved by a factor  $(n)^{1/2}$ . The general statement may be made that the energy gain in a linear accelerator is proportional to the square root of the product of the RF power input and the accelerator length. This conclusion applies to a single section made up of a multiplicity of cavities; it applies also to a long accelerator consisting of a multiplicity of sections.

The distribution scheme just discussed is possible in principle but difficult in execution. The design and construction of a feed system to provide equal amounts of power per cavity and to achieve the desired phase relationship between cavities would be quite complex.

Consider another system wherein the structure simultaneously serves the functions of accelerator and waveguide. Consider first an ordinary cylindrical waveguide excited in the  $TM_{01}$  mode, as shown in Fig. 5-8. If the guide is properly terminated, there will be a wave traveling in one direction in the guide which could conceivably be used for the acceleration of electrons since it has an axial component of electric field. The difficulty is that this wave has a phase velocity greater than the velocity of light,  $c$ , and material particles such as electrons cannot exceed  $c$ . Thus, being unable to keep up with the wave, they would drop behind and receive no net acceleration.

There are various ways of slowing down the phase velocity of the wave. The method used at Stanford consists of periodically loading the waveguide with metal disks, as shown in Fig. 5-9. When this structure is excited as before, it is now observed that as the excitation frequency is varied there are an infinite number of pass bands separated by attenuation bands. At a particular

**Figure 5-8**  
Cylindrical cavity excited in  $TM_{01}$  mode.



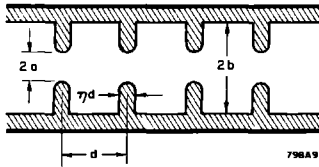


**Figure 5-9** Disk-loaded cylindrical waveguide.

frequency there are also an infinite number of wave components, each traveling at a characteristic phase velocity. These additional components are required to satisfy the boundary condition imposed by the addition of the disks. The loading can be adjusted until one component is traveling at the desired phase velocity, typically the velocity of light. If this component is the one of which the velocity is closest to the phase velocity in the unloaded guide, this particular component will contain the largest share of the total RF energy, about 90%. The RF energy carried by the other wave components is wasted in the sense that it does not contribute to the useful acceleration of electrons. These components, with velocities different from those of the electrons, give rise to oscillatory forces which average to zero in a long accelerator.

Another feature of a linear electron accelerator which is important to understand is the question of orbit stability. It might be assumed that getting the electrons to pass through a pipe  $\frac{3}{4}$ -in. in diameter and 2 miles in length is an insurmountable problem. Even if the pipe were absolutely straight, it is virtually impossible to aim the electron gun at the beginning of the machine so accurately that the electrons will pass through such a small pipe. Fortunately these problems are not real for two reasons. First, the supposed difficulty is not based upon accurate reasoning because the effects of relativity have been neglected. According to the theory of relativity, an observer traveling with the electrons would see the pipe greatly foreshortened. However, the transverse dimensions of the accelerator are not altered, so that the  $\frac{3}{4}$ -in. hole retains the same dimension regardless of the axial electron velocity. Figure 5-10 indicates the degree of foreshortening of the accelerator. For example, if the machine is 10,000 ft long, then at an energy of 15 GeV it appears to the electron to be only 42 in. long. The problem of getting an electron through a hole  $\frac{3}{4}$ -in. in diameter and 42 in. long is a trivial one—at least as compared to the precision needed in presenting an accurate picture on the screen of a television picture tube.

Further, the straightness of an accelerator is not a critically important matter because relatively simple means can be used to redirect the electrons if a small bend in the pipe occurs. Beam position monitor devices sense the deviation of the beam from the axis of the accelerator and display this information for the operator. The operator then adjusts the current in simple dipole steering coils spaced along the accelerator to deflect the beam as needed, thus causing it to remain centered in the accelerator.



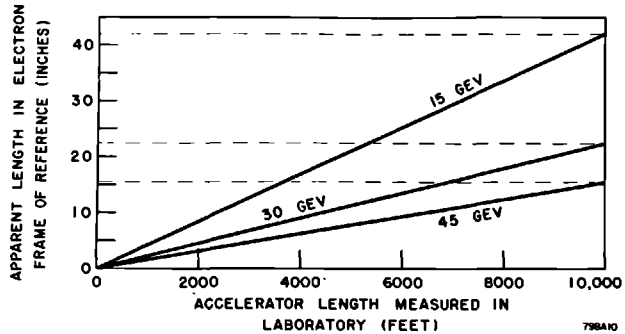


Figure 5-10 Apparent length in electron frame of reference compared to actual accelerator length.

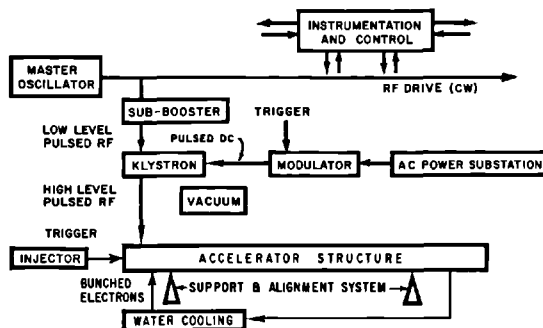
### 5-4 Accelerator components and systems

A block diagram illustrating the principal components and systems of the two-mile accelerator is shown in Fig. 5-11. Most of these units are repeated many times in the entire accelerator length. For example, there are 960, 10-ft long accelerator sections, 245 klystrons, 245 modulators, 30 sub-booster klystrons, 30 power substations, and 30 vacuum systems. The instrumentation and control system is spread over the entire accelerator length, although the machine can be operated from a single Central Control Room.

#### Accelerator structure

The accelerator proper is a cylindrical, copper, disk-loaded structure in which an axial electric field traveling at the velocity of light is set up when the structure is excited with microwave power at a frequency of 2856 MHz. The structure is designed to produce a constant axial electric field over the length of each independently fed, 10-ft section. This constant gradient characteristic is achieved by suitable variation of the modular dimensions of the section. The shunt impedance of the structure is approximately 53 megohms/meter, which

Figure 5-11 Accelerator components and systems.



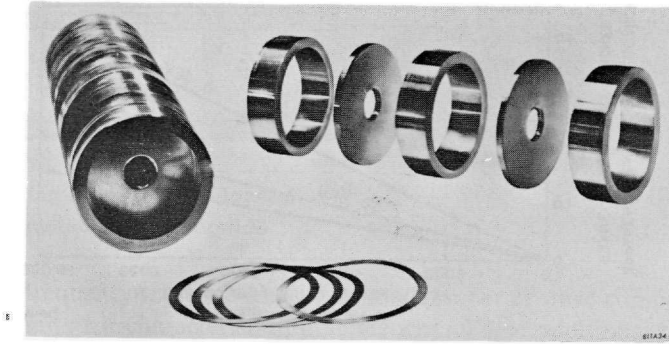
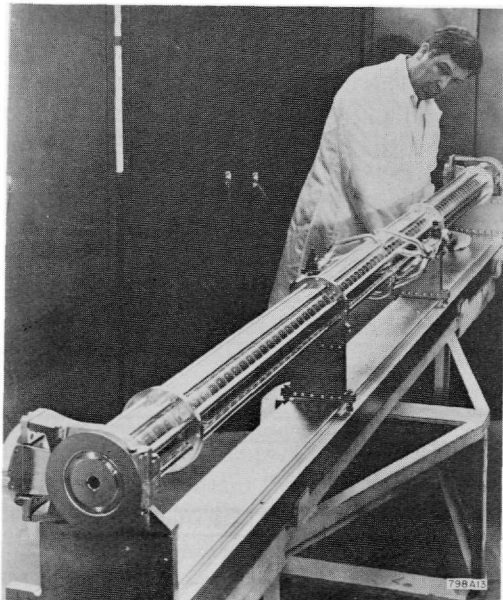


**Figure 5-12** Accelerator disks and cylinders.

results in an electron energy gain in million electron volts in a 10-ft section of  $\approx 10 P^{1/2}$ , where  $P$  is the input RF power to the section in megawatts.

The accelerator structure was fabricated by a brazing technique from the basic disk and cylinder elements shown in Fig. 5-12. These parts were independently machined to accuracies of  $\pm 0.0002$  in. They were then carefully stacked and clamped together on a stainless steel mandrel passing through the disk apertures. Brazing was accomplished in a special flame furnace which provided a reducing atmosphere both inside and outside of the structure to prevent oxidation. A completed 10-ft section is shown in Fig. 5-13.

**Figure 5-13**  
View of completed 10-ft accelerator section.



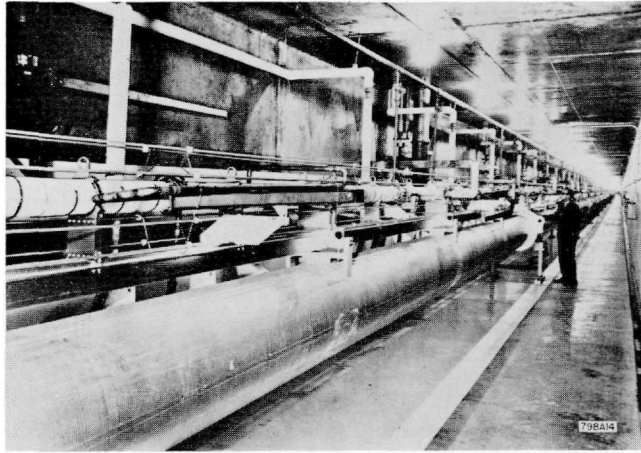


**Figure 5-14** Installed basic 40-ft accelerator modules each consisting of four 10-ft sections mounted on a 24-in. diameter aluminum girder.

Four of the 10-ft sections are mounted on a 40-ft aluminum girder, 24 in. in diameter. This is the modular length of the accelerator for support and alignment purposes. The aluminum girder serves dual functions as support for the accelerator and as a “light pipe” for alignment purposes. The assembled and installed girders are shown in Fig. 5-14.

### *Alignment system*

Each of the 40-ft support points of the accelerator is aligned with respect to a straight line defined by two end points. One of the end points is a laser light source located at the end of the accelerator near the beam switchyard and the other end point is a slit with a photomultiplier detector located upstream from the main injector. The laser light source provides a beam of light which is transmitted through the 24-in. aluminum support girder. The girder (light pipe) is evacuated to a pressure of about  $10^{-2}$  torr to reduce refraction due to temperature gradients in the residual gas. At each 40-ft support point, a retractable Fresnel target, as shown in Fig. 5-15, images the light source on the detector. The transverse location of the image indicates the deviation of the target from its correct position. The jacks at the corresponding support point can be adjusted to bring the target into correct alignment. The correct angular rotation of the accelerator is assured by the use of precision level devices. The system described is able to align the accelerator to  $\pm 0.5$  mm. A separate laser, located in the beam switchyard, is provided to align the switchyard components using the same detector as the accelerator alignment system.

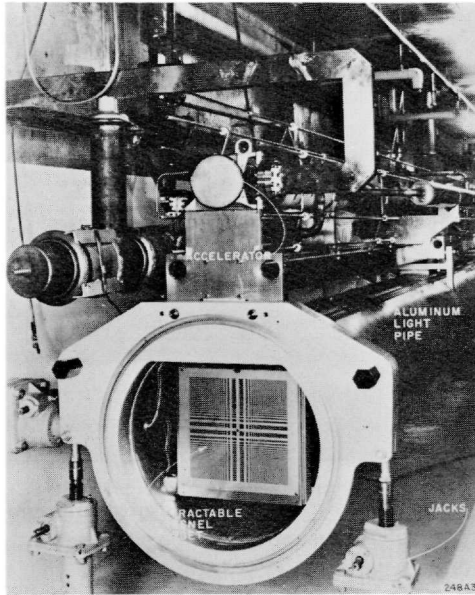
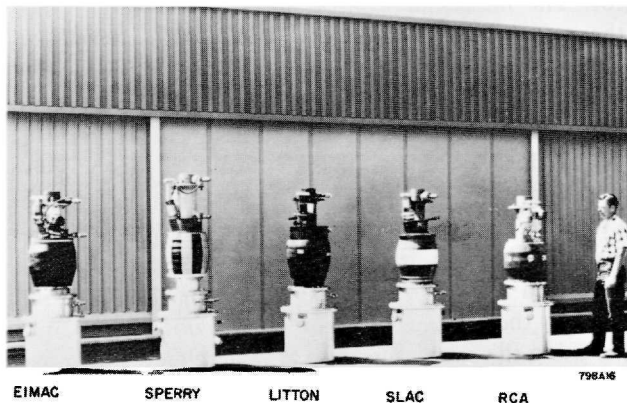


Figure 5-15 End of 40-ft girder showing retractable Fresnel target.

### *Klystrons*

The RF power sources are high-power klystron amplifiers. A basic tube having a design capability of 24 MW peak and 22 kW average power was developed at SLAC. Four commercial companies also developed tubes for the accelerator meeting the same basic specifications as the SLAC tube. A group photograph of the five different tubes is shown in Fig. 5-16. All these

Figure 5-16 Klystron models manufactured by SLAC and by four commercial companies.



EIMAC

SPERRY

LITTON

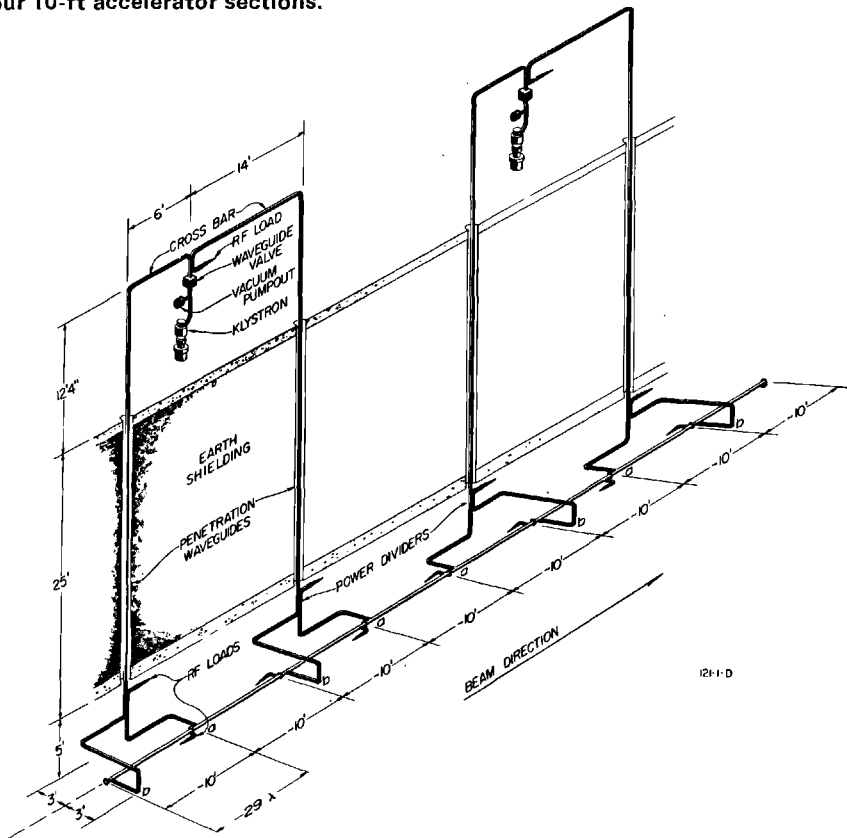
SLAC

RCA

tubes have permanent magnet focusing and are electrically and mechanically interchangeable. The use of permanent magnet focusing instead of the more customary electromagnetic focusing eliminates the need for water cooling of the focusing system and for focusing power supplies. It also results in simplification of the interlock system.

The power from each klystron is divided four ways (Stage I) and is used to supply power to the four 10-ft sections located on a single 40-ft girder. The general arrangement of the klystron, the connecting waveguides, and the accelerator sections is shown in Fig. 5-17. Waveguide feeds to the accelerator connect to opposite sides of successive sections to compensate for deflecting forces due to residual coupler asymmetries. The provision of a waveguide valve just above each klystron allows the klystron to be replaced without affecting the accelerator vacuum or interfering with beam operation. If the Stage II modification is later undertaken, the number of klystrons will be increased to 960 so that each klystron will feed a single 10-ft section.

**Figure 5-17** General arrangement of klystron, connecting waveguide, and four 10-ft accelerator sections.



The klystron and its associated pulse transformer tank are designed to be suspended from a special support yoke. This simplifies the installation of the tube and its alignment with the rectangular waveguide system.

### *High-power modulators*

Each klystron amplifier is provided with a "line-type" modulator rated at 65 MW peak and 75 kW average power, a pulse length of 2.5  $\mu$ sec, and a maximum pulse repetition rate of 360 pulses/sec. The pulse-forming network in the modulator is discharged through a single hydrogen thyratron capable of handling the entire peak and average power requirements—the voltage of the output pulses from the modulator is increased by a factor of 12 by means of a pulse transformer, and the resulting pulses at a voltage of 250 kV (maximum) are then applied to the associated klystron.

Each modulator is provided with a "de-Q'ing" circuit which compares the charging voltage of the pulse network during each charging cycle to a reference voltage. When the level of the charging voltage reaches the reference level, the energy stored in a charging transactor is dumped into a dissipative circuit by means of a silicon-controlled rectifier switch. This effectively clamps the charging voltage at the reference level and thus stabilizes the output pulses from the modulator to  $\pm 0.1\%$  even in the presence of significant (approximately  $\pm 3\%$ ) variations in the ac line voltage.

All sixteen modulators located in each pair of 333-ft sectors are provided with power from a variable voltage substation located in the klystron gallery. The input power to each substation is provided at a 12.47-kV level by means of underground cables from the master substation located near the east end of the accelerator. The output voltage of the substation is remotely controlled over a range of 258 to 595 volts ac from the Central Control Room. All of the sixteen modulators connected to the substation receive the same voltage. However, different substations can be operated at different output voltage levels.

### *Injector system*

A diagram of the main injector is shown in Fig. 5-18. It is designed to inject a well-bunched ( $5^\circ$ ) and well-collimated beam of electrons into the accelerator. Since the energy gain of an accelerated electron is proportional to the cosine of the phase angle that it occupies with respect to the peak of the traveling RF wave, good bunching of the electrons is essential in order to attain a narrow, electron energy spectrum at the output of the accelerator. The electron gun which operates at 80 kV is of the triode type which permits the pulse length and beam current to be selected on a pulse-to-pulse basis from any of three predetermined sets of values. This feature of the injector, together with the ability to trigger the klystrons in the various sectors in time with or after the beam (or at various repetition rates), permits carrying on several simultaneous experiments in the research areas at different incident energies, pulse

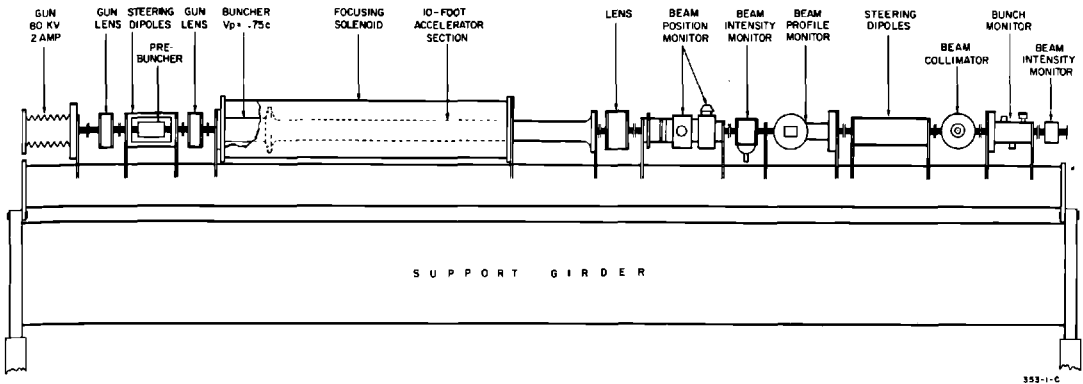


Figure 5-18 Profile view of injector.

lengths, and intensities. The prebuncher consists of a velocity modulation cavity. The bunching section is a disk-loaded section 10.5 cm long in which the phase velocity is 75% of the velocity of light. It serves to reduce the phase spread by a factor of 2.5 (while increasing the momentum spread by the same factor) and increases the beam energy to 260 keV. A 10-ft long, constant gradient, accelerator section increases the energy to approximately 30 MeV. For phase synchronization, the prebuncher, buncher, and 10-ft accelerator section are all driven by power from the same klystron, which is conservatively run at half to two-thirds of its power capability to give good life and stability.

A special beam knockout device is used when there is a need to increase the time (and space) separation of the electron bunches. This is desirable, for example, when carrying out certain experiments utilizing time-of-flight techniques. Removal of the unwanted bunches is accomplished by means of sinusoidal, transverse electric fields. These varying fields, which are developed between metal deflecting plates, deflect some of the bunches right or left into the accelerator walls while allowing other bunches to pass through undeflected. One set of these plates is located in the injector system between the prebuncher and the buncher. These plates are supplied with RF power at 39.667 MHz (the 72nd subharmonic of the 2856-MHz power which accelerates the electrons). One electron bunch passes through undisturbed at each voltage null. All other bunches are deflected and are thus effectively removed from the beam. Since two nulls occur during each cycle, one bunch out of every thirty-six entering the deflecting system survives and is accelerated through the entire machine. The peak current in this bunch can be increased until the average current in the beam is nearly equal to the maximum achievable when all of the bunches are present.

The 39.667-MHz drive power originates in one of the lower-frequency stages of the master oscillator. It is amplified by a special pulsed modulator before being applied to the deflecting plates. Other frequencies can, of course, be applied to achieve various desired spacings of the bunches. A second set

of beam knockout plates is provided for at the end of the first accelerator sector in case it is desired to reduce the phase extent (longitudinal size) of the bunch to a further degree. This second knockout stage can also serve to remove any "dark current" which may originate in the first sector. Dark current arising in later sectors can easily be eliminated in the magnetic slit system located in the beam switchyard.

### *Drive and phasing systems*

The klystron amplifiers must receive coherent low level signals at 2856 MHz so that the RF waves in the accelerator sections will have the correct frequency and phase relationships with the individual bunches of electrons passing through the accelerator. The RF drive system consists of

- a master oscillator providing 476-MHz power;
- a main booster amplifier which increases the 476-MHz power to 17.5 kW, continuous wave;
- a  $3\frac{1}{8}$  in. diameter main drive line 2 miles long;
- couplers and varactor frequency multipliers at each 333-ft sector which remove a small portion of the main drive signal and multiply the frequency by 6 to 2856 MHz;
- a pulsed sub-booster klystron at each sector that amplifies the 2856-MHz power by 60 dB;
- a  $1\frac{1}{8}$ -in. diameter coaxial line which transmits 2856-MHz drive power to the vicinity of each of the high-power klystrons in the sector;
- couplers that remove approximately 4 kW peak. After attenuation, 300 watts remain to drive each klystron.

The main drive signal is transmitted at the subharmonic frequency, 476 MHz, because the low loss at this frequency ( $\approx 0.25$  dB/100 ft) permits transmission over 2 miles without series boosters which, if used, would lead to phase shift and reliability problems.

The RF phasing system uses the phase of the electron bunches in the accelerator as the phase reference. It is based on the principle that the wave induced by the bunched electron beam in an accelerator section is  $180^\circ$  out of phase with respect to the wave from a correctly phased klystron supplying power to that section. Phasing is accomplished automatically (within  $\pm 5^\circ$ ) by sectors when initiated by the operator.

### *Vacuum system*

The all-metal high vacuum system capable of maintaining the accelerator and waveguides at  $< 10^{-6}$  torr is shown schematically in Fig. 5-19. One such system is provided for each 333-ft sector. Four 500-liter/sec getter-ion pumps located in the klystron gallery evacuate the accelerator and waveguides through interconnecting stainless steel manifolds. A pump can be removed



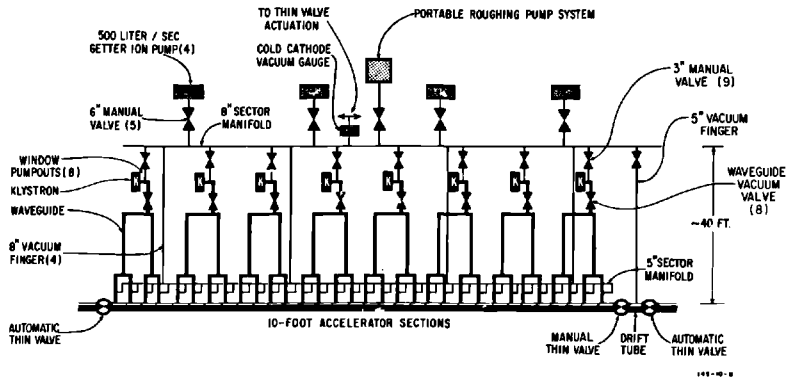


Figure 5-19 Vacuum system schematic for one 333-ft sector.

for servicing without interference with accelerator operations by closing the associated 6-in. valve. Similarly, an individual klystron can be replaced by closing the 3-in. valve connecting it to the pumping manifold and the waveguide vacuum valve in its output RF system.

Separate pumping systems are provided for rough-pumping the accelerator, for the 24-in. light pipe, and for the beam switchyard.

### Cooling water systems

Most of the electrical energy consumed by the accelerator components is eventually absorbed by the cooling water systems. In addition to absorbing power, these systems serve to regulate the temperatures of critical components such as the accelerator tube, the rectangular waveguides, the RF drive line, and the klystrons.

The water systems utilize secondary loops which include the devices being cooled and primary loops containing outside cooling towers which transfer heat to the atmosphere. Heat is transferred from the secondary to the primary loops through shell-and-tube heat exchangers.

The cooling water systems are the accelerator tube cooling water system, the waveguide-drive line cooling water system, and the klystron cooling water system.

Control of accelerator tube temperature is necessary to maintain the phase velocity of the electromagnetic wave in the accelerator equal to the velocity of light. The phase shift  $\delta\theta$  between the electrons and the wave in a 10-ft section is given by  $\delta\theta = 2Q\tau k \delta T$ , where  $Q$  = the unloaded  $Q$  of the accelerator cavities ( $\approx 13,000$ ),  $\tau$  = attenuation parameter ( $\approx 0.57$ ),  $k$  = thermal coefficient of expansion of copper ( $\approx 8.9 \times 10^{-6}/^\circ\text{F}$ ), and  $\delta T$  is the deviation in the temperature of the accelerator structure. Thus,  $\delta\theta \approx 7.5^\circ$  for  $\delta T$  equal to  $1^\circ\text{F}$ . The accelerator tube cooling water system provides each 10-ft accelerator section with 13 gal/min. The input temperature of the cooling water

to each sector is manually adjusted to a value  $[113 - 0.6 P_{AV}(\text{kW})] \pm 0.2^\circ\text{F}$ , where  $P_{AV}(\text{kW})$  is the average RF power input to the 10-ft accelerator sections of that sector. It has been empirically determined that this input water temperature will result in the design temperature of  $113^\circ\text{F}$  in the metal walls of the accelerator. As an example, for  $P_{AV}(\text{kW}) = 4 \text{ kW}$ , the correct input water temperature is  $113 - (0.6)(4) = 110.6^\circ\text{F}$ . Control of the input temperature of the cooling water manually is adequate for all sections which receive one-quarter of the output power of a klystron. This is the case for the vast majority of the accelerator sections. However, for those 10-ft sections in the injector and in the first sector of the accelerator, each of which receives all the power from one klystron, it is necessary to adjust the temperature of the input water over a range of about  $13^\circ\text{F}$ . This adjustment is made automatically so that, with the varying temperature gradients caused by changing equilibrium heat flow, the temperature of the accelerator wall remains constant. Thus, the input water temperature varies between  $100^\circ$  and  $113^\circ\text{F}$ , the lower input temperature corresponding to maximum power flow from the klystron to the accelerator section.

Except for the special constant metal temperature cases just discussed, a separate temperature-control loop is provided for each accelerator sector.

To prevent phase shift in the rectangular waveguides and in the drive lines, these lines are provided with 5 and 10 gal/min, respectively, of cooling water at a temperature of  $112 \pm 1.0^\circ\text{F}$ . There is one temperature-control loop per sector.

The major sources of heat in the entire installation are the klystron amplifiers. These tubes each have a maximum rating of 75 kW of average power. Under normal conditions, about 60% of this power is dissipated in the tube itself. To prevent overheating, each tube is provided with 11 gal/min at a supply temperature of  $95 \pm 1^\circ\text{F}$ . There are ten separate temperature-controlled circuits, one for every three sectors.

Each of the secondary cooling water loops is provided with a bypass demineralizer unit around its circulating pump. The accelerator tube and waveguide-drive line loops also have filters in these bypass lines. The klystron loops have full flow filters in the pump suction line.

Two large cooling towers located at approximately  $\frac{1}{2}$  mile and  $1\frac{1}{2}$  miles along the 2-mile housings serve to remove the heat from the primary loops. The flow in each cooling tower loop is 500 gal/min with two of the three pumps operating. In typical operation, the supply temperature is  $75^\circ\text{F}$  and the return temperature is  $90^\circ\text{F}$  at  $68^\circ\text{F}$  (wet bulb).

### *Positron source*

A positron beam has to be delivered to the main experimental stations at the end of the accelerator for positron scattering experiments and the creation of a monochromatic photon beam by annihilation with electrons. In addition, a positron beam will be required at the two-thirds point along the

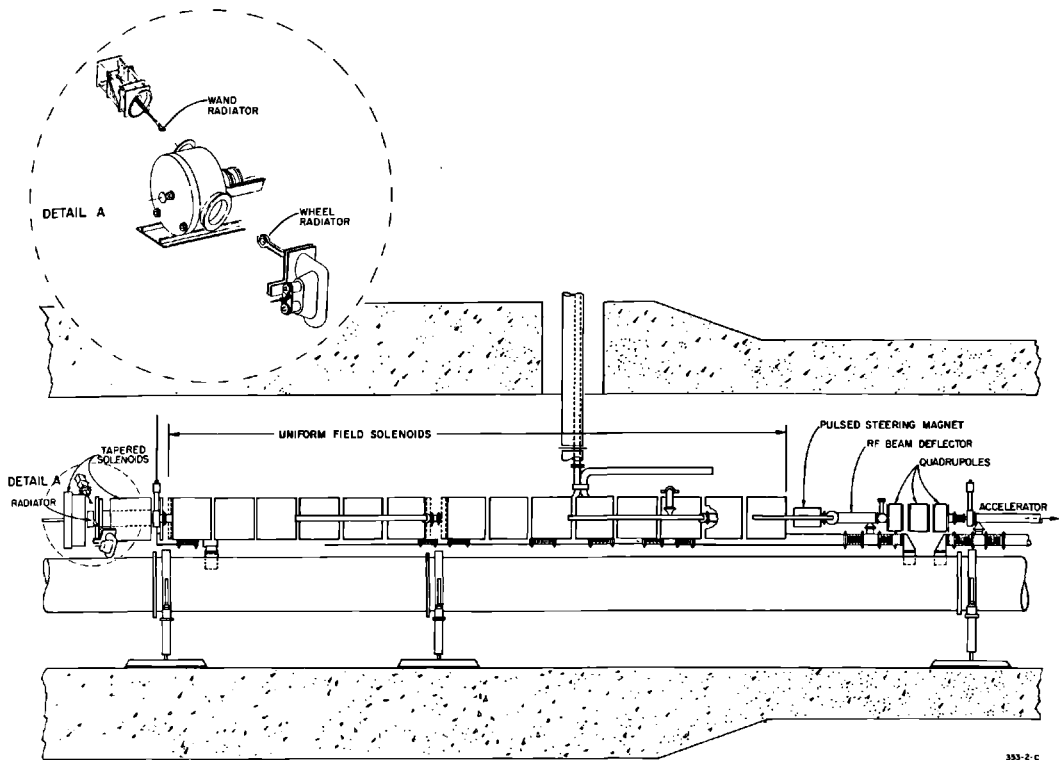


**Figure 5-20** Positron source and its associated focusing and instrumentation equipment.

accelerator for injection into a proposed positron–electron storage ring. The beam is created at the one-third point along the machine by inserting a target and reversing the RF phase of the first one-third of the accelerator. With 100 kW of incident electron beam power, a positron current of approximately  $0.45 \mu\text{A}$  ( $7.5 \times 10^9$  positrons/pulse)\* can be accelerated in an energy band of about 1% and a transverse phase space of approximately  $0.15 \pi(\text{MeV}/c)(\text{cm})$ .

The positron source system is shown in Fig. 5-20. Either of two separate radiators can be inserted into the beam. Each radiator has a thickness of about 4 radiation lengths of copper. A “wand” radiator is provided for intermittent positron pulses at rates up to 4 pulses/sec. It is a small target, 0.38 in. wide, driven across the beam line on command in a time equivalent to about 9 machine pulses (at 360 pulses/sec). The center pulse of this group results in a positron pulse; the other eight are suppressed by gating the main injector. All other pulses may be transmitted as a normal electron beam, if

\* The maximum current actually achieved to date (July 1967) is about one-third of this amount (see Chapter 16).

desired. The second radiator is in the form of a "trolling" water-cooled wheel. It is used when continuous positron production is desired.

A magnetic lens system is used to improve the match between the source emittance and the accelerator phase space acceptance. The radiator is located in a 20-kG axial magnetic field which decreases rapidly to 2.4 kG about 2 ft downstream of the radiator and then remains constant for the next 24 ft. Acceleration begins 2.5 ft downstream of the radiator, and the positron energy at 25 ft is about 75 MeV, at which point the solenoidal focusing is replaced by a series of thirteen quadrupole triplets and doublets of which the spacing increases with energy until this focusing system merges with the regular machine doublet system located at the end of each sector.

A pulsed RF deflector located downstream of the target is used to produce an angular deflection of the positron and electron beams. Because the beams are  $180^\circ$  apart in phase, they are both deflected by the same angle. Thus, depending on which beam is needed, a magnetic dipole can be used to restore the direction of either the positron or the electron beam to the axis while deflecting the other even farther.

### *Instrumentation and control*

**CONTROL LOGIC.** For purposes of control, the two-mile accelerator is divided into thirty sectors. Each sector has an instrumentation alcove which serves as a data collection and transmission point. These alcoves are not manned except during maintenance or for diagnosis of troubles.

The number of signals and controls for the entire machine is so large that one operator, or even several operators, could not attend to them if they were all available simultaneously. For this reason, a system of summary alarm signals has been provided to alert the operator as to which sector requires attention. The operator can then switch a sector control panel to the sector in question. This panel displays the complete set of analog and status information for that sector and also connects the remote control system to the same sector.

The system is designed for initial control by human operators. However, the signal format has been arranged so that a control computer can be added at a later date for purposes of data logging, beam steering, and energy control.

**DATA TRANSMISSION SYSTEM.** Some of the data developed along the two-mile accelerator is needed only locally by maintenance personnel for periodic adjustment, diagnosis, or data logging purposes. Most of these types of data are associated with equipment which is relatively quiescent, i.e., a given status or adjustment of such equipment is ordinarily maintained for relatively long periods. Detailed operating conditions on this type of equipment are not reported to the Central Control Room (CCR) but out-of-tolerance performance is usually reported by means of a summary alarm signal.

Other data are so critical to operations that precise quantitative transmission and display at central control are essential. Examples of such data are *steering dipole current* and *sector vacuum*. Such data are transmitted as dc analog signals with a range of 0 to 5 volts on an individual wire pair. The signal is displayed at CCR on a 2% accurate, panel voltmeter. Noise pickup and cable leakage are low enough to permit display with 0.1% accuracy if a high grade meter is employed. Each circuit is grounded at only one point, usually one terminal of the voltage source. Each of the thirty accelerator sectors is provided with twenty analog signals for transmission of data to CCR.

Other information needs to be transmitted only as status signals, which are two-valued functions. For example, it may be sufficient to know whether a certain device is on or off, or within or outside a preset tolerance. Each sector is provided with 100 status channels which are time-division multiplexed and transmitted to CCR on a single wire pair as a binary-coded, frequency-shifted signal. Information is updated twice each second.

After every accelerator pulse, beam intensity and beam position signals derived from a microwave system at each sector are multiplexed and transmitted to CCR as a succession of three pulses on a single wire pair. These pulses are proportional to the  $x$  and  $y$  displacements of the beam from the axis and to the logarithm of the charge in the beam pulse. The logarithm of charge rather than the charge itself is used as a basis so that a wide dynamic range can be transmitted. However, the accuracy is correspondingly decreased (to about  $\pm 30\%$ ). A separate accurate ( $\pm 1\%$ ) signal proportional to charge in a beam pulse is derived from a toroidal coil in each sector drift section and transmitted to CCR by means of a precise FM (20–40 kHz) transmitter. The four beam-monitoring signals from each sector, along with similar signals from other sectors, are multiplexed in succession onto four oscilloscopes in CCR presenting beam intensity and position information to the operator for the entire two-mile accelerator.

Similar beam-monitoring signals as well as beam energy and spectrum information are transmitted to CCR from the beam switchyard.

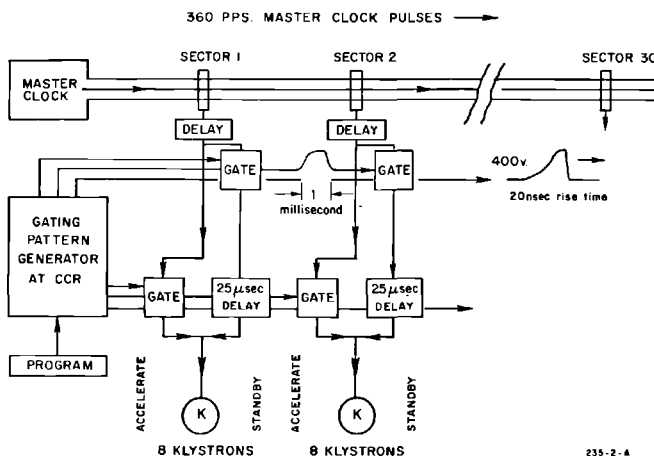
**REMOTE CONTROL SYSTEM.** Most of the remote controls for accelerator equipment are actuated by an economical binary system. Three sector control panels in CCR each contain switches, status lights, and analog meters governing the most important control functions applicable to any sector. By depressing a switch, the operator can connect any one of the three panels to control any one of the thirty sectors. The transmission system for remote control consists of six parallel binary wire-pair channels, which are capable of selecting  $2^6$  different control functions at a sector. A seventh wire pair transmits the actual binary control command. The same seven wire pairs are bridged from sector to sector for the entire length of the machine. A separate wire pair to each sector provides means to switch the controls to a particular sector.

TRIGGER SYSTEM. Although the basic repetition rate of the accelerator is 360 pulses/sec, the trigger system permits operation of various accelerator sectors and other subsystems in a very flexible manner so that up to six beams having distinct energies, currents, and destinations in the research area can be programmed. The repetition rates of these beams can be adjusted to be any value between 1 and 360 pulses/sec. The trigger system is illustrated in Fig. 5-21. Clock pulses at 400-volt level and 360 pulses/sec are sent over the entire 2 mile length along a single,  $1\frac{1}{8}$ -in. diameter, coaxial cable. A small amount of power is removed from the main line by means of couplers at each station (e.g., injector, accelerator section, positron source) and is sent to the local trigger generator. A gating pulse is sent to each local trigger generator from the pattern generator in central control. Since the time precision ( $\approx \pm 5$  nsec) is inherent in the clock pulses, the gating pulses do not have to be very precise and can be transmitted on ordinary wire pairs.

In Fig. 5-21, the pattern generator pulses are shown gating the clock pulses admitted to the klystron modulators of each sector. If a particular sector is not to contribute to the energy of a particular beam, the pattern gating signal causes the modulators to be triggered 25–50  $\mu$ sec late, after the beam pulse has been transmitted through the sector. In other arrangements, the pattern signals may cause a particular sector to pulse at a lower repetition rate, such as 60, 120, or 180 pulses/sec.

BEAM GUIDANCE AND DIAGNOSTIC EQUIPMENT. To compensate for the earth's magnetic field and for stray ac and dc fields along the machine, parallel degaussing wires and concentric magnetic shielding are provided, reducing the average fields below  $10^{-4}$  G. The degaussing currents are independently adjustable for each sector. The magnetic shielding material consists of 0.006-in. thick, molybdenum-permalloy material which results in a local shielding

Figure 5-21 Trigger system block diagram.



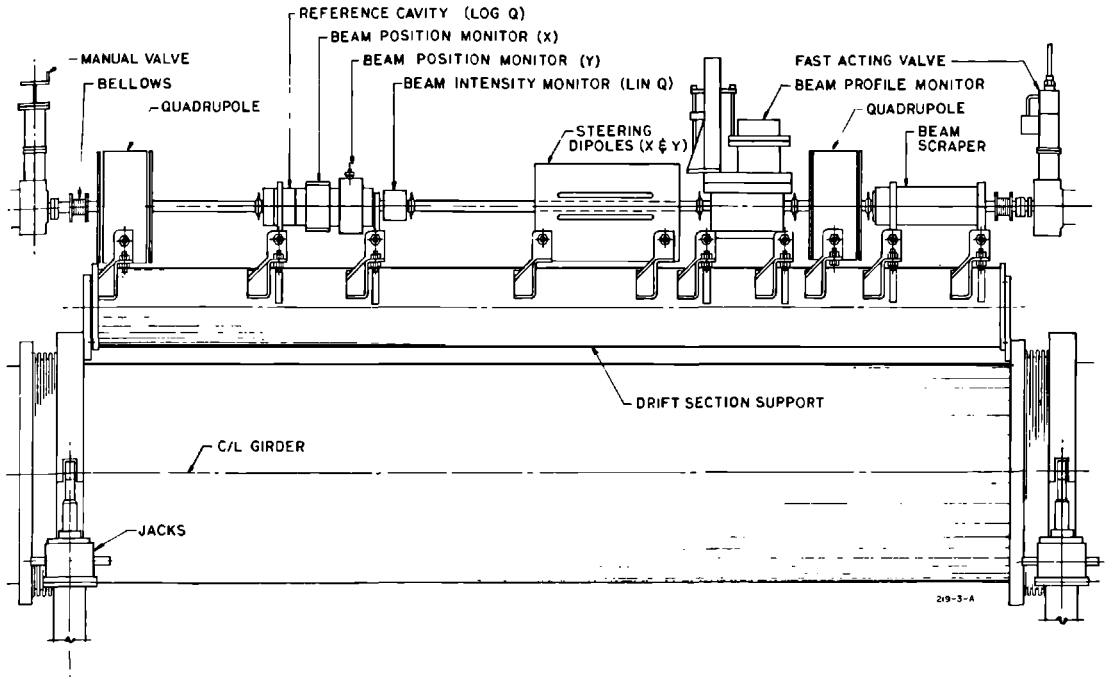


Figure 5-22 Standard instrument section located at end of each 333-ft sector.

factor of about 30 and an overall effective value of about 10, considering unavoidable gaps.

Beam monitoring, steering, and focusing devices are provided in a 10-ft drift section at the end of each 333-ft sector of the accelerator. The layout of a standard drift section is shown in Fig. 5-22. Equipment in this section consists of a quadrupole doublet, steering dipoles (X and Y), a phase reference cavity, beam position monitors (X and Y), a beam intensity monitor, a beam profile monitor, and a "beam scraper" (collimator). The beam position monitor consists of two rectangular cavities which are excited in the  $TM_{120}$  mode by an off-axis beam. Since the phase of the excitation depends on the direction of beam deviation from the axis, the sense of the deviation can be detected by comparing the phase of the wave from the beam position monitor cavities with the phase of the wave from the phase reference cavity which is excited in the  $TM_{010}$  mode. Beam positions accurate to better than 1.0 mm are displayed in central control from thirty such systems.

A long ion chamber consisting of a  $1\frac{5}{8}$ -in. coaxial line, filled with a mixture of argon and carbon dioxide, running the full length of the accelerator housing is provided to inform the operator regarding beam losses. From the times of arrival of the ionization signals at the injection end of the accelerator it is possible to resolve the position of the beam loss within 100 to 200 ft. The

ion chamber signal display provides a good profile of the accelerator's radiation due to beam loss. In addition, the injector is automatically turned off in case the beam loss signal at any point exceeds a preset threshold.

**PERSONNEL RADIATION PROTECTION SYSTEM.** Interlocking of the personnel accessways to the potentially dangerous radiation areas is the primary means of radiation protection. Opening of any of these entrances results in turning off the variable voltage substations providing power to the klystrons and also turning off the injector. The design of the protection system has to take into consideration the fact that there are approximately 100 entrances to radiation areas spread out over the entire site.

Red and green lights in the klystron gallery inform personnel when the klystrons are operating. Access to the gallery is controlled at two gates in the peripheral fencing rather than at the 150 doors of the gallery itself. Since radiation in the gallery is principally from the klystrons and is nominally quite low, the access points to the gallery are not interlocked with the electron beam or with the power supplies.

The personnel protection system consists of three major parts: the *machine shut-off system*, which prevents turn-on until the radiation areas are cleared and secured and which turns off the machine in case the security of any area is broken; the *access control system*, which prevents entry into radiation areas while the machine is on; and the "Emergency Stop" circuit which inserts beam stoppers in appropriate positions when excessive radiation is detected in the research area. In addition, the system contains warning devices and radiation monitors to help determine the state of the machine.

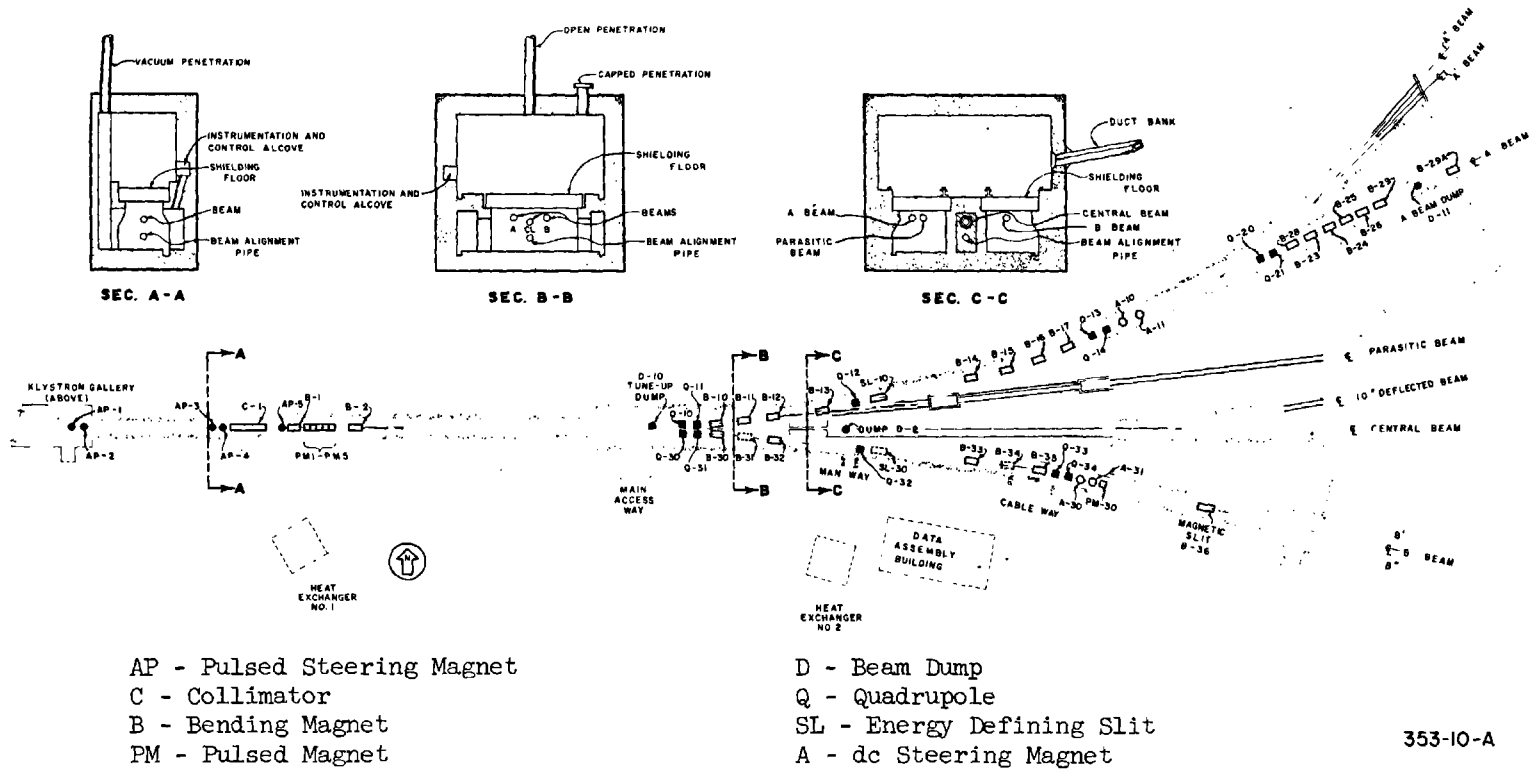
The machine shut-off system is based upon the integrity of double tone loops (40 and 50 kHz) which redundantly determine when the security of any radiation area is broken. If either tone loop is interrupted, all variable voltage substations and the injector are automatically turned off. If the shut-off system is tripped, the area in the vicinity of the open interlock must be searched and a reset button within the area must be actuated. Simultaneous acknowledgment by the CCR operator is required to complete the reset process. Interlocks in the shut-off system are operated from batteries so that momentary interruptions of ac power need not destroy the housing security.

The access control system contains a tone loop which is closed only if all the variable voltage substations are turned off. Only if this loop is closed can the operator release keys from the keybanks to allow personnel to enter the radiation areas.

## 5-5 Beam switchyard

A layout of the beam switchyard is shown in Fig. 5-23. This is a large two-level underground structure covered by 40 ft of concrete and earth for radiation shielding purposes. The beam path itself is located on the lower level. The upper level contains utility runs, instrumentation and control alcoves,





353-10-A

Figure 5-23 Beam switchyard plan.

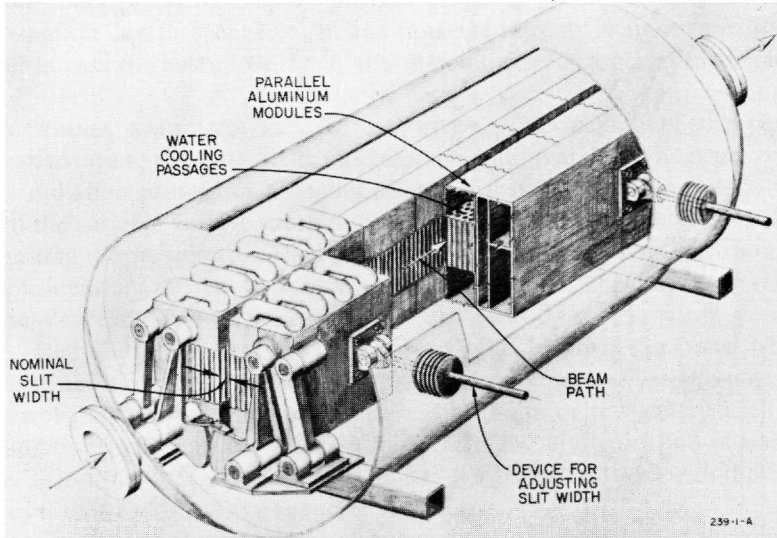


**Figure 5-24**  
**High-power energy-defining slit located in beam switchyard.**

cranes, service cars, and ancillary equipment for the main beam transport devices in the lower level.

By use of a pulsed magnet system which deflects the electrons (or positrons) on a pulse-to-pulse basis into any of three large dc magnet transport systems, it is possible to carry out several experiments simultaneously in the research area using time-interlaced beams.

The unusually high-power ( $\approx 1$  MW in Stage I) carried by the incident beam has imposed very difficult problems in the design of the beam handling equipment. A typical example of a device capable of handling these large beam powers is the 16-ft long, adjustable, energy-defining aluminum slit shown in Fig. 5-24. Two in-line slits of the type shown, with the second rotated  $90^\circ$  about its axis with respect to the first, are used as an adjustable collimator at the beginning of the beam switchyard.

A small, digital, process control computer (SDS 925) is used in the control system of the beam switchyard. This computer reads data from punched cards and sends digital control information to regulators in the magnet power supplies where digital-to-analog converters generate analog reference voltages. Slits and collimators are adjusted in a similar way. When desired by the operator or experimenter, data representing the parameters of a particular beam are printed out from the computer memory for record, together with auxiliary information. About 100 signals from various sources are scanned every accelerator pulse (1/360 sec) and about 600 signals are scanned at a slower rate. The computer detects, identifies, and prints out the time and date of any changes in the interlock and status signals in proper sequence.



work, the primary beam creates photons in a thin target in the beam switchyard and is then deflected downward and absorbed in the "A-beam dump" located near the east end of the switchyard. This dump is isolated from end station A by thick steel shielding.

The "counting house," containing electronics equipment used in conjunction with End Station A experiments, is located in a shielded room adjacent to and immediately west of the end station at a level about 50 ft above the floor of the experimental hall. End Station A contains three spectrometers, rated at 20, 8, and 1.6 GeV/c, which are used to measure the angles and momenta of particles resulting from interactions of incident electrons or positrons with target nuclei. This area also includes (immediately east of end station A) a 2-meter streamer chamber for use in photoproduction experiments.

Large openings have been provided in the walls of end station A to permit extension of experimental equipment to the concrete pad exterior to the building if needed. When these openings are not in use they are covered with thick portable shielding blocks.

The second existing research area centers around end station B, where experiments concerned with the creation of secondary particles and determination of their characteristics are performed.

Because creation of secondary beams involves the impingement of a high-power primary beam on suitable targets, a separate well-shielded target room is provided between the beam switchyard and end station B. Ports for the passage of the secondary beam into end station B are provided in the shielding wall. As in the case of end station A, openings are provided in the outer walls of end station B to permit extension of experimental equipment to the concrete pad outside of the building, if desired. At the present time, three beams have been constructed in the end station B area: a muon beam, a neutral K beam, and a monochromatic gamma beam. Two major instruments used in these experiments are a 1-meter hydrogen bubble chamber and a spark chamber with its associated 54-in. magnet.

Both end stations A and B are provided with heavy duty cranes capable of handling equipment or shielding weighing up to 50 tons.

A third (central) experimental area includes an 82-in. hydrogen bubble chamber which has been moved from Lawrence Radiation Laboratory, Berkeley.

## 5-7 Initial operating results

### *Key dates*

Perspective regarding the operating results obtained to date may be gained from an examination of the "key dates" given in Table 5-2.

An early plan called for construction of a prototype length of the machine (one or two sectors) to verify and test the mechanical, electrical, and

Table 5-2 Key dates

April 1957	Proposal for two-mile accelerator
September 1961	Authorization by Congress
April 1962	Contract with AEC
January 1965	1.5-GeV beam through two sectors
April 21, 1966	Beam to two-thirds point (Sector 20)
May 21, 1966	Beam through 30 sectors to beam switchyard
June 2, 1966	18.4-GeV beam in beam switchyard (tune-up dump)
September 16, 1966	Beam to A-beam dump in beam switchyard
September 20, 1966	Beam to research area A and beam dump east
November 1, 1966	Beam to research area B
December 20, 1966	Accelerated $e^+$ beam from positron source
January 10, 1967	20.16 GeV achieved
March 29, 1967	240 kW of average beam power into A-beam dump

instrumentation design features. This plan was not followed because of the associated high costs and difficulty of fitting this subproject into the design and production schedules. Instead of building separate prototype sectors, the completion of the first two sectors (666 ft) of the accelerator was pushed ahead of the rest. By January 1965 it was possible to accelerate a 1.5-GeV beam through these two sectors. As a result of these tests<sup>2</sup> a number of important but not fundamental changes were made in the remaining sectors. Sectors 1 and 2 were later modified to correspond to the other sectors in most respects.

It was decided after these first tests to move the beam-analyzing station originally located at the end of Sector 2 to a new location near the beginning of Sector 20. Recent operating experience has proved that this relocation was wise in that it has permitted testing up to two-thirds of the machine with a beam even when the beam switchyard is unavailable as a result of installation or maintenance activities.

The beam was first accelerated through all thirty sectors on May 21, 1966. A beam energy of approximately 10 GeV was obtained at that time. Less than 2 weeks later, on June 2, 1966, the energy was increased to 18.4 GeV by turning on more klystrons at somewhat higher levels and by better phasing of the available klystrons.

On September 20, 1966, a beam was run for the first time to Research Area A and to beam dump east (beyond end station A). The beam was first sent to end station B on November 1, 1966, and the experimental program on the B side started immediately after this date.

On December 20, 1966, positrons were first accelerated from the positron source at the one-third point in the accelerator housing to beam-analyzing station No. 2 at the two-thirds point.

The two most recent achievements shown in Table 5-2 are concerned with maximum energy and maximum beam power. On January 10, 1967, a beam

energy of 20.16 GeV was obtained with all but four of the klystrons participating. On this occasion, the klystrons were operated about 5% below their rated voltage level. On March 28, 1967, a beam having an average power of 240 kW was transmitted to the A-beam dump. The corresponding parameters were an energy of about 17 GeV, a peak current of 25 mA, 1.6  $\mu$ sec beam pulse length, and a repetition rate of 360 pulses/sec.

*Beam characteristics: energy, spectrum, loading, and power*

The electron energy gained in the multisection accelerator of constant gradient design is given by

$$V = (1 - e^{-2\tau})^{1/2} \sum_n (P_n l r)^{1/2} - \frac{irNl}{2} \left( 1 - \frac{2\tau e^{-2\tau}}{1 - e^{-2\tau}} \right)$$

where

- $N$  = number of independently fed sections
- $l$  = length of each section
- $P_n$  = input RF power to section  $n$
- $r$  = shunt impedance per unit length
- $i$  = peak beam current
- $\tau$  = RF attenuation per accelerator section in nepers

The first term in this equation is the "no-load" energy, i.e., the energy for negligible beam current. The second term accounts for the energy decrease caused by beam loading. Inserting the design parameters of the SLAC accelerator ( $N = 960$ ,  $l = 3.05$  meters,  $r = 53$  megohms/meter, and  $\tau = 0.57$  nepers) into the above equation and considering the fact that each klystron feeds its power equally into four accelerator sections and that some of the power ( $0.54 \pm 0.1$  dB) is dissipated in the waveguides connecting the klystrons to the accelerator, the result is

$$V_{\text{GeV}} = 0.020 \sum_n P^{1/2} - 0.035i$$

with  $P$  measured in megawatts and  $i$  in milliamperes. This equation is plotted in Fig. 5-26 for the case where the outputs of all klystrons are assumed to be the same and equal to 21 MW. In this case, the no-load energy is seen to be 22.0 GeV. The beam energy decreases from the no-load value at the rate of 35 MeV/mA (independent of input power levels). Also shown in the same figure is the average beam power obtained by multiplying the above energy equation by the peak beam current and then by the beam duty cycle. Theoretically, the power transferred to the beam is maximum when the peak current is such that the beam energy is reduced to one-half of the no-load value, i.e., in this case to 11 GeV. The peak current corresponding to maximum average beam power ( $\approx 2.1$  MW in this example) is equal to approximately 312 mA.

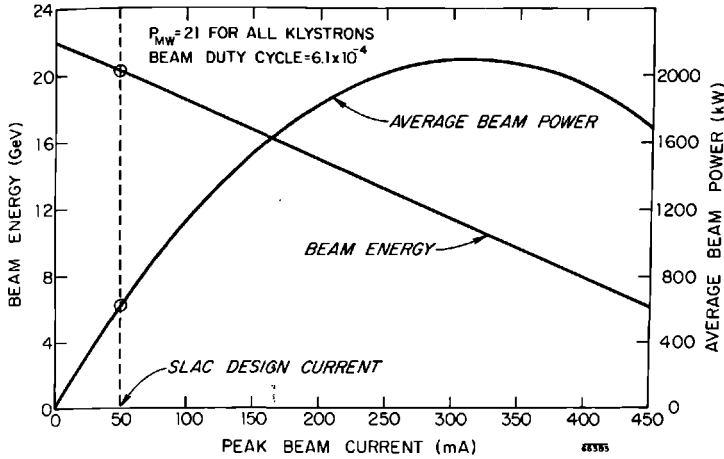
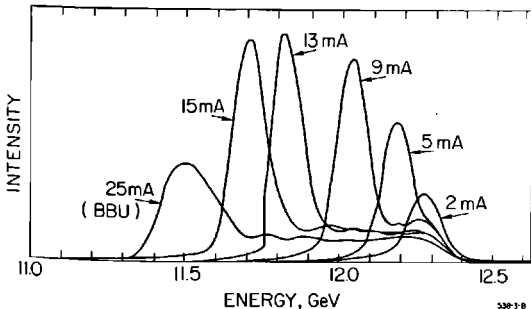


**Figure 5-26** Beam energy and average beam power vs peak beam current for the SLAC accelerator.

The design current and the corresponding design energy and average beam power for the SLAC accelerator are 50 mA, 20 GeV, and 600 kW, respectively. These design values are indicated in Fig. 5-26. Design values of beam current and beam power were not initially achieved because of the onset of beam breakup phenomena as discussed in a later section. However, the coefficients in the energy design equation were verified within experimental accuracy (about 2%).

Typical energy spectra are shown in Fig. 5-27. The highest-energy spectrum resulted from relatively light beam loading ( $i = 2.0$  mA). A large beam current ( $i = 25$  mA) led to a beam having 0.80 GeV less energy. The low-energy spectrum is broader than the high-energy spectrum due to the presence of electrons in a high-energy tail. This tail is due to those electrons that

**Figure 5-27** Energy spectra under different beam loading conditions.



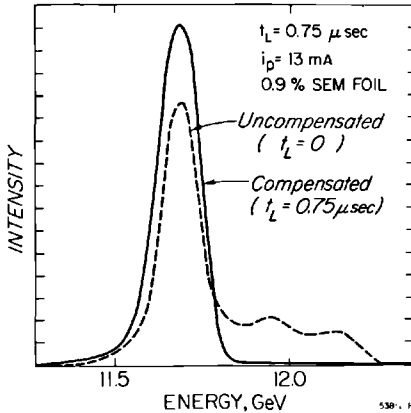


**Figure 5-28 Compensation of spectrum broadening due to beam loading by trigger delay to one sector.**

pass through the accelerator early in the beam pulse before the beam has extracted a significant amount of stored RF energy. Broadening of the spectrum in this manner is usually undesirable in physics applications of the beam. One useful method of compensating for this effect consists of delaying the time of triggering one or more of the accelerator sectors. When this is done, the first electrons during the pulse pass through the sector when it is not completely filled with RF energy and therefore gain less than the maximum energy potential. Later electrons encounter a situation where the sector is completely filled but some of the stored energy has been extracted by the pioneering electrons. By proper adjustment of the trigger delay to the sector, it is possible to achieve near equality in the energies of the earlier and later electrons. Compensation obtainable with this technique is indicated in Fig. 5-28 where the dotted curve represents the uncompensated spectrum and the full curve is the compensated spectrum achieved by trigger delay to one sector.

The spectrum width at half-maximum for the cases shown in Fig. 5-27 is approximately 1.3%, of which about 0.9% is attributable to resolution of the measurement devices. In more recent runs with careful adjustment of beam parameters, spectra with widths of  $\approx 0.2\%$  have been obtained.

#### *Beam transmission*

Careful measurements have shown that more than 90% of the beam current measured at beam-analyzing station No. 1, located at the 40-ft point, is preserved during passage through the entire machine. This favorable result arises from the effective performance of the beam position and intensity monitors, the steering and focusing systems, and the long ion chambers.

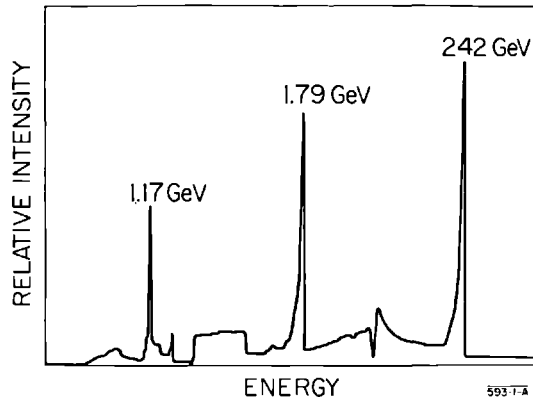


The microwave position monitors located in the drift space at the end of each sector are capable of indicating the transverse position of the beam within  $\pm 0.5$  mm.

Beam optics measurements at beam-analyzing station No. 1, located 40 ft from the injector, have shown that 80% of the injected beam is contained in a transverse phase space of  $1.2 \times 10^{-2}$  (MeV/c)(cm). A second measurement in the beam switchyard at the end of the accelerator indicates that the same fraction of the beam is contained in a transverse phase space of about  $3 \times 10^{-2}$  (MeV/c)(cm). Since the beam diameter at that point is roughly 0.4 cm, the angular divergence of the beam in the energy range of 10 to 20 GeV is less than  $10^{-5}$  radian.

Tests to date have demonstrated the capability of accelerating at least three beams in a time-interlaced manner. Spectra of three low-energy interlaced beams measured at beam-analyzing station No. 2 in Sector 20 are shown in Fig. 5-29. Independent control of the energy, intensity, and pulse length of each beam is feasible. This capability permits the simultaneous performance of several independent experiments in physically separated areas. The trigger "pattern" for these beams is selected by the operator in the CCR and is sent to the appropriate destinations, namely the injector, the accelerator sectors, the beam switchyard pulsed magnets, and the experimental areas. The beam intensity presentation observed by the operator for two interlaced beams of energies 11 and 5.65 GeV is shown in Fig. 5-30. Two base line traces are shown. The height of each dot above the corresponding base line is proportional to the beam intensity at the end of a particular sector. These signals originate from toroid-type intensity monitors located in the drift space at the end of each sector. Similar displays are viewed by the operator to ascertain the vertical and horizontal beam position relative to the accelerator axis at the end of each sector. In this instance, all dots lie

**Figure 5-29 Spectra of three time-interlaced beams.**



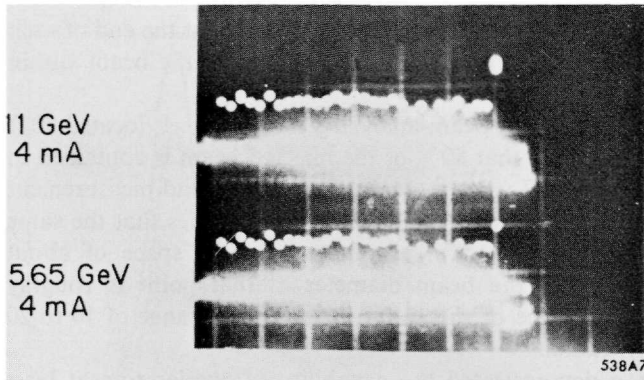


Figure 5-30 Beam intensity at end of each sector for two interlaced beams.

on the base line when the beam is perfectly centered. Displacement of a dot above or below the base line implies a right or left, or upward or downward displacement of the beam from the axis.

#### *Beam breakup and remedial measures*

Beam breakup phenomena originally limited the maximum peak current through the entire two-mile accelerator to approximately 20 mA at the maximum energy gradient. This was about 40% of the design current level. Higher currents can be accelerated to intermediate points along the accelerator. Furthermore, the maximum current transmitted to a given position along the accelerator can be increased by reducing the beam pulse length. Lower-energy gradients lead to reduced threshold current levels. In general, the product

$$\frac{it_p z}{\delta V/\delta z} \approx \text{constant}$$

where  $i$  is the peak beam current at which beam breakup occurs,  $t_p$  is the length of the beam pulse as limited by breakup,  $z$  is the distance from the injector to the closest position where current is lost at time  $t_p$  during the beam pulse, and  $\delta V/\delta z$  is the average energy gradient in the accelerator.

While the current originally available was adequate for all initially scheduled experimental purposes, it was realized that some future experiments would probably require higher current. Therefore, means of increasing the beam breakup current threshold were incorporated in the accelerator.

The most significant improvement has resulted from strengthening the focusing along the accelerator. The original focusing system consisted of thirty quadrupole triplets, with one triplet being located in the drift section at the end of each 333-ft accelerator sector. In addition, thirteen special triplets were used for focusing positrons produced by the positron source at the

one-third point along the accelerator. Each triplet consisted of a collinear set of two A-type quadrupoles at the ends of the drift section and one B-type quadrupole in the center. The B quadrupoles are twice as long as the A quadrupoles and, thus, for a given current have twice the focusing strength. Originally, triplets were chosen rather than doublets because calculations showed that they would introduce less steering error in the presence of short-term misalignments due to thermal effects in the support structures. However, actual measurements with the completed accelerator showed that misalignment effects are so small that doublets can be used without difficulty. This permitted rearrangement of the quadrupoles as follows:

1. Removal of all of the longer (B) quads from Sectors 1 through 29 and from the special positron triplets.
2. Installation of doublets consisting of B-type quadrupoles in the drift sections of Sectors 10 through 29. Procurement of larger regulated power supplies capable of 15 A output for these doublets.
3. Installation of doublets consisting of A-type quadrupoles in the drift sections of Sectors 1 through 9, using standard power supplies (7 A maximum current).
4. Installation of the remaining A-type quadrupoles as singlets between 40-ft girders in the first six sectors, using standard power supplies.

With the quadrupole arrangement just described, it was possible to taper the quadrupole current linearly from Sectors 1 through 29 so as to obtain the same effective betatron wavelength for the electron orbits over the entire accelerator length. Previously, it had been possible to taper only up to 7 A quadrupole current. When the plan just discussed was completed it was possible to taper up to a normalized value of 30 A. These measures resulted in an increase of peak beam current to the value of 42 mA.

In addition to the straightforward or "brute-force" technique described above, other schemes for increasing the beam breakup thresholds are being studied. These include microwave filtering and injector noise reduction schemes. Work in these areas is still preliminary and no significant progress can yet be reported.

### *Klystron status and performance*

Among the principal accelerator components, klystrons are being singled out for special review because of their significant role in accelerator performance and reliability and their high cost. Because of these factors, the early decision was made to procure these tubes from several sources so that there would always be backstops against technical and production difficulties involving one or two vendors. In addition, SLAC itself chose to fabricate a reasonable number of the production tubes both for insurance purposes and also to afford a ready means of developing and testing improved models of klystrons.

**Table 5-3 Klystron status as of July 27, 1967**

<i>Vendor</i>	<i>Total contract</i>	<i>Accepted</i>	<i>Installed</i>
RCA	216	205	98
Sperry	80	80	3
Litton	144	114	90
SLAC	54	54	49
Litton <sup>a</sup>	6	6	3
Eimac <sup>a</sup>	6	5	2
<b>Total</b>	<b>506</b>	<b>469</b>	<b>245</b>

*Note:* 245 klystrons are required to fill all accelerator sockets.

<sup>a</sup> Special 6 tube contract.

A total of 245 klystrons is required to fill all the sockets along the accelerator. These tubes are rated at 21 MW peak and 21 kW average power output. Their design capability is somewhat higher than these ratings.

The status of klystron procurements and the SLAC in-house program as of July 1967 is given in Table 5-3. These procurements did not all start at the same time. Tubes from all sources are designed to be repairable. Thus, the total number of tubes being procured allows both for a quantity sufficient to fill the repair cycle and to provide a suitable reserve. SLAC has negotiated an extended warranty agreement with two of the vendors wherein, after initial purchase of a tube, SLAC pays in addition a fixed hourly rate for the first 1500 (or 2100) hours of operation of the tube and a decreased rate thereafter. Under this arrangement, the manufacturer agrees to replace a failed tube with a tube meeting original specifications at no additional acquisition cost to SLAC. The fixed hourly rate cycle described above then applies to the replacement tube.

Klystron operating experience through June 30, 1967 is summarized in Table 5-4. Tube operating hours are given by quarter and cumulatively. Also given are the number of failures and average life at failure on both a quarterly and a cumulative basis. In terms of the cumulative values, one klystron failure has occurred for each 7600 operating tube hours. This is, of course, not an accurate measure of tube life expectancy except after many generations. An attempt to predict mean life on the basis of the present meager experience is shown in Fig. 5-31, where age at failure for each tube has been plotted against the percentage of tubes which have failed. The horizontal scale is constructed so that a normal failure distribution will result in a straight line when life at failure is plotted as indicated above. The data plotted omit all failures of the tubes of one of the manufacturers since the failure rate for this company is about twelve times the average failure rate for the other two

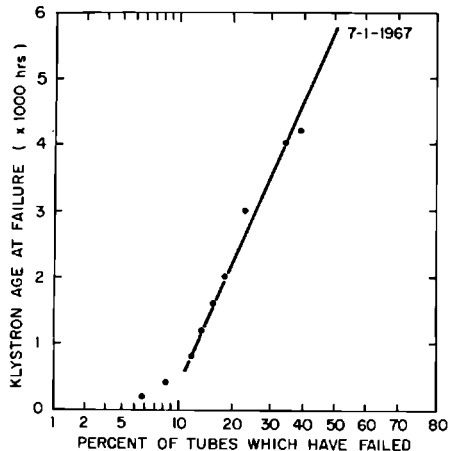
**Table 5-4 Klystron usage and failure**

<i>Dates</i>	<i>Operating hours</i>		<i>Quarter</i>		<i>Cumulative</i>	
	<i>Quarter</i>	<i>Cumulative</i>	<i>No.</i>	<i>Avg. life at failure</i>	<i>No.</i>	<i>Avg. life at failure</i>
To 12/31/65	—	27,000	—	—	10	297
To 3/31/66	11,000	38,000	13	252	23	272
To 6/30/66	118,000	156,000	16	234	39	256
To 9/30/66	127,000	283,000	15	594	54	350
To 12/31/66	176,000	459,000	23	1070	76	575
To 3/31/67	228,000	687,000	28	1670	104	860
To 6/30/67	301,000	988,000	26	2166	130	1130

companies and SLAC. Where the line crosses the 50% failure coordinate, the corresponding mean time to failure may be read on the vertical scale. The predicted mean time to failure from this data is approximately 5700 hours. A better prediction of tube life must await more operating results.

SLAC has continued to do development work on klystrons during the construction and operating periods. Recently, an experimental SLAC klystron, when operated at a beam voltage of 300 kV, produced a peak power output of 42 MW with an efficiency of 45%. Although tubes having these improved characteristics are a long way from production, this result indicates that at some time in the future a significant increase in power output of production klystrons may be possible. Many questions relating to stability and life must, of course, first be resolved.

**Figure 5-31  
Klystron failure experience.**



*Operating statistics*

Statistics for the first year of operation (FY 1967) are shown in Table 5-5 and Fig. 5-32a and b.

The total manned hours include not only operating shifts but also shifts during which the machine was shut down for scheduled maintenance, equipment modifications, and search activities. The total number of klystron hours is  $\int N(t) dt$ , where  $N(t)$  is the number of klystrons in use at a given time  $t$ . Allowing about 5% reserve, approximately thirteen klystrons are needed at 1 mA beam current for each gigaelectron volt of beam energy. Thus, the number of klystron hours depends not only upon the total hours of operation but also upon the average beam energy. As noted in Table 5-5, a total of 833,413 klystron hours were run in FY 1967. This is an average of 3400 hours for each of the 245 klystron sockets on the accelerator.

The total productive beam hours given in Table 5-5 is the number of hours the accelerator was operated with one or more useful beams. Accelerator beam tuneup time and other nonproductive beam time has been excluded. The total experimental hours include actual beam hours and beam downtime requested by the experimenters. This total includes the sum of the operating times of simultaneous experiments.

Figure 5-32a shows how the total hours of manned shift time were divided during each month of the fiscal year. The accelerator was shut off for extensive installation and maintenance work during the weeks of October 23–29, December 25–31, January 1–7, February 5–11, and May 28–June 3 which explains some of the decreases in useful beam time. Figure 5-32b shows the percentage times devoted to the various activities on a quarterly basis. It is significant to note that the fraction of the manned shift time utilized for particle physics increased from 0 in the first quarter to 58.1% in the last quarter of FY 1967. During the same interval, the time devoted to machine

**Table 5-5 Operating statistics for FY 1967**

Manned hours	5,700
Klystron hours	833,413
Total productive beam hours	2,874
Low energy (<3 GeV)	709
Machine physics	698
Particle physics	11
High energy	2,165
Machine physics	493
Particle physics	1,672
Total experimental hours	3,466
Machine physics	1,342
Particle physics	2,124

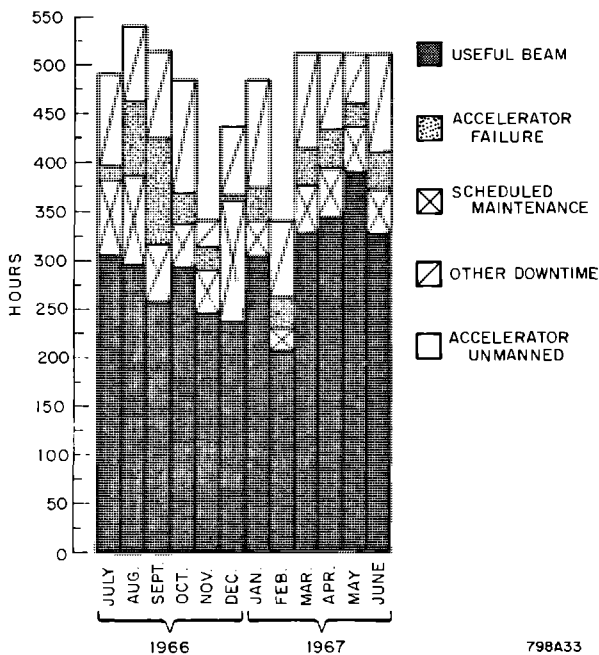


Figure 5-32a Operating statistics, hours per month.

